Universidad de Concepción
Dirección de Postgrado
Facultad de Agronomía
Programa de Doctorado en Ciencias de la Agronomía

CARBONO ORGÁNICO DEL SUELO, PREDICCIÓN DE SU TASA DE DESCOMPOSICIÓN EN EL MARCO DEL CALENTAMIENTO GLOBAL.
(SOIL ORGANIC CARBON, PREDICTION OF ITS DECOMPOSITION RATE IN THE CONTEXT OF GLOBAL WARMING.)

Tesis para optar al grado de Doctor en Ciencias de la Agronomía

MARCELA ANDREA HIDALGO GIUBERGIA
CHILLÁN-CHILE
2022

Profesor Guía: Erick Zagal Venegas
Dpto. de Suelos y Recursos Naturales, Facultad de Agronomía
Universidad de Concepción

Esta tesis ha sido realizada en el Departamento de Suelos y Recursos Naturales de la Facultad de Agronomía, Universidad de Concepción.

Profesor Guía

Dr. Erick Zagal Venegas
Ingeniero Agrónomo, M.Sc., PhD

Comisión Evaluadora

Dra. Cristina Muñoz Vargas
Ingeniero Agrónomo, Dr. Cs. Rec. Nat.

Dr. Leandro Paulino
Ing. Forestal; M Cs., Dr. Cs.

Dr. Marco Matías Pfeiffer Jakob
Ingeniero Agrónomo, M.Sc., PhD

Directora de Programa

Dra. María Dolores López Belchi
Facultad de Agronomía
Universidad de Concepción

Dedicado a: Iñaki, Catalina y Agustín Serra Hidalgo, Ignacio Serra, Corina Giubergia, Pierino Giubergia, Norma Quezada, Katherine Rebolledo y a mis queridos amigos y familiares que me han apoyado.

RECONOCIMIENTOS

Al Proyecto Regular Fondecyt N°1161492 y al Programa de Doctorado en Ciencias de la Agronomiá de la Facultad de Agronomía de la Universidad de Concepción.

AGRADECIMIENTOS / ACKNOWLEDGMENT

A mi Profesor Guía: Dr. Erick Zagal, por su confianza y apoyo, por motivarme a obtener este grado y por su apoyo a través del trabajo y experiencia laboral, sin duda ha sido un Mentor que me ha enseñado mucho de la ciencia y la vida.

Al Dr. Sebastian Doetterl, Profesor Colaborador Internacional (ETH-Zürich, Department of Environmental Systems Science, Zürich, Switzerland), por su apoyo, enseñanzas y su confianza en mi.

A la Srta Katherine Rebolledo, Ténico Análista del laboratorio, quien me ayudó más allá de la preparación de las muestras y análisis en el laboratorio. Sino que también con su amistad y apoyo emocional en minutos difíciles durante el desarrollo del doctorado.

Al Sr. Juan Fuentes, Técnico Agrícola por su apoyo en el muestreo y en los años que trabajamos juntos, llegando a ser un gran amigo.

A la Sra. Gloria Sepúlveda por su ayuda, amistad y legado en mineralogía de suelos.

A mi familia por su amor e incondicional apoyo, especialmente a mis hijos Iñaki, Catalina y Agustín, A Ignacio por creer en mi. A mi madre por su apoyo, cuidar y amar a mis hijos. A mi hermana Daniela por su apoyo, A mi nonno por su amor y retarme siempre para que terminara el doctorado, mi nonna por responder a mis plegarias.

A mis amigos por apoyarme, escucharme, salir a la montaña, apoyar a mis hijos y animarme.

Finalmente a todos quienes han formado parte de mi vida en este periodo.

TABLA DE CONTENIDOS

ÍNDICE DE FIGURAS Y TABLAS

CAPÍTULO 2.

NEAR-INFRARED SPECTROSCOPY: ALTERNATIVE METHOD FOR ASSESSMENT OF STABLE CARBON ISOTOPES IN VARIOUS SOIL PROFILES IN CHILE

CAPÍTULO 3.

PREDICTING SOIL ORGANIC CARBON STABILIZATION AND TURNOVER USING $\delta^{13}C$ IN DEPTH PROFILES, ASSESSED BY NEAR INFRARED SPECTROSCOPY, UNDER PERMANENT GRASSLAND ALONG A LATITUDINAL TRANSECT IN CHILE

CARBONO ORGÁNICO DEL SUELO, PREDICCIÓN DE SU TASA DE DESCOMPOSICIÓN EN EL MARCO DEL CALENTAMIENTO GLOBAL.

SOIL ORGANIC CARBON, PREDICTION OF ITS DECOMPOSITION RATE IN THE CONTEXT OF GLOBAL WARMING.

Palabras adicionales: Near-infrared spectroscopy, Carbon isotope abundance, $\delta^{13}C$, C mineralization rate, latitudinal transect, specific potential respiration, soil profiles.

RESUMEN

La descomposición del carbono (C) en el suelo depende de complejas interacciones entre variables ambientales que difieren a lo largo de gradientes latitudinales. El objetivo de esta investigación fue evaluar y validar un modelo predictivo para los valores de ^{13}C utilizando espectroscopia de infrarrojo cercano (NIRS) en varios perfiles de suelo, para probar la aplicabilidad de un índice de mineralización y respiración del C orgánico del suelo (COS) basado en valores NIRS de $\Delta\delta^{13}C$. Trece sitios en praderas naturales de vegetación C3 se muestrearon a lo largo de un gradiente latitudinal de 4000 km (30° a 50°S) en Chile, maximizando la diversidad climática y geoquímica del suelo. En un primer estudio se evaluó NIRS para la determinación de isótopos estables de C del suelo y para un escrutinio rápido de múltiples muestras. Por lo tanto, inicialmente se determinó el valor de $\delta^{13}C$ de las muestras mediante espectrometría de masas de relación isotópica, frente al estándar Pee Dee Belemnite de Viena y mediante el escaneo en el rango NIR y a una resolución de 4 cm^{-1}. Dos modelos de

predicción basado en valores NIRS $\delta^{13}C$ fueron desarrollados a través de la regresión parcial por mínimos cuadrados (RPMC) usando diez latentes variables y un enfoque de bosque aleatorio (BA). El error cuadrático medio de predicción para la validación de las simulaciones de $\delta^{13}C$ obtenidos usando RPMC y BA fueron 1.38‰ y 1.15‰, respectivamente. El desempeño de ambos modelos indica que NIRS puede ser usado para predecir $\delta^{13}C$ según el set de datos seleccionados. Luego, en un segundo estudio, se realizaron incubaciones a diferentes profundidades de suelo por 60 días, para evaluar las tasas de mineralización de C del suelo (TMC) y la respiración potencial específica (RPE) como indicadores de la descomposición de C, utilizando la variación de la firma de NIRS $\delta^{13}C$ (modelo RPMC) a medida que aumenta la profundidad del suelo ($\Delta\delta^{13}C$). En su totalidad, los resultados de esta investigación apoyan el uso de la NIRS como método predictivo en los análisis sobre la dinámica del C en el suelo. A su vez, $\Delta\delta^{13}C$ obtenido a partir de datos NIRS pueden servir como proxy para investigar la degradabilidad potencial de la MOS y su interacción con los procesos geoquímicos.

ABSTRACT

Carbon (C) decomposition in soil depends on complex interactions between environmental variables that differ along latitudinal gradients. The objective of this investigation was to evaluate and validate a predictive model for ^{13}C values using near-infrared spectroscopy (NIRS) on several soil profiles, to test the applicability of an index of soil organic C mineralisation and respiration (COS)

based on NIRS values of $\delta^{13}C$. Thirteen sites in natural grasslands of C3 vegetation were sampled along a 4000 km latitudinal gradient (30° to 50°S) in Chile, maximising climatic and soil geochemical diversity. In a first study we tested NIRS to assess stable isotopes of C in soil for fast screening of multiple samples. Therefore, initially the $\delta^{13}C$ value of the samples was determined by isotope ratio mass spectrometry against the Vienna Pee Dee Belemnite standard and scanned in the NIR range at a resolution of 4 cm^{-1}. Two prediction models based on NIRS $\delta^{13}C$ values were developed through partial least squares regression (PLS), using ten latent variables, and a random forest (RF) approach.The root mean square error of prediction for the validation runs for $\delta^{13}C$ obtained using the PLS and RF models were 1.38‰, and 1.15‰, respectively. Both model performances indicate that NIRS can be used to predict $\delta^{13}C$ for the selected dataset. Then, in a second study, incubations were conducted at different soil depths for 60 days to assess soil C mineralisation rates (CMR) and specific potential respiration (SPR) as indicators of C decomposition, using the variation of the NIRS $\delta^{13}C$ signature (PLS model) with increasing soil depth ($\Delta\delta^{13}C$). Overall, the results of this research support the use of NIRS as a predictive method in analyses of soil carbon dynamics. In turn, $\Delta\delta^{13}C$ obtained from NIRS data can serve as a proxy to investigate the potential degradability of SOM and its interaction with geochemical processes.

I. CAPITULO 1. INTRODUCCIÓN GENERAL Y OBJETIVOS

1. INTRODUCCIÓN.

Las emisiones de gases invernadero han aumentado en forma dramática a partir de la revolución industrial, especialmente debido al uso de energías de origen fósil y al cambio de uso de suelo asociado a actividades agrícolas, de transporte e industriales (IPCC, 2013). El dióxido de carbono (CO_2) es uno de los principales gases de efecto invernadero (GEI) que juegan un rol importante en los procesos del cambio climático. En las últimas décadas este fenómeno ha sido estudiado por investigadores en diferentes disciplinas, los cuales han predicho un incremento en la temperatura de la atmósfera y los océanos debido principalmente a la emisión de los GEI tales como CO_2, metano, óxido nitroso, ozono y clorofluorocarbonos (IPCC, 2013). El suelo representa el segundo reservorio más importante de C orgánico del planeta, con un contenido estimado de 1.500 a 1.700 Pg (1 Pg = petagramo = 1 billón de toneladas) a una profundidad de 100 cm. Esto corresponde al doble de la concentración de CO_2 en la atmósfera (730 Pg) y cerca de tres veces lo que se encuentra en la vegetación (500 Pg) (Powlson et al. 2012). Sin embargo, el C secuestrado en el suelo, podría convertirse en una fuente de emisión de CO_2 como consecuencia del calentamiento global (Reay and Grace, 2007; Lal, 2006; Davidson and Jansses, 2006). Bajo este contexto, un cambio en la tasa de descomposición de la materia orgánica del suelo, debido a un aumento en la temperatura del suelo como consecuencia del calentamiento global, podría convertir al suelo (y pasar

de ser un reservorio de C) en una fuente de emisión de CO_2, contribuyendo a un mayor calentamiento del planeta. La distribución global del C orgánico del suelo (COS) es heterogénea y depende del tipo de suelo, la actividad microbiana del suelo, el uso de la tierra y las limitaciones climáticas. A escala mundial, nuestra comprensión de los procesos de estabilización y descomposición del C del suelo, así como de los factores que los controlan, sigue siendo limitada.

1.1. El suelo como fuente o emisor de CO_2 atmosférico y los efectos del clima y componentes geoquímicos del suelo en el flujo suelo-atmósfera.

El intercambio anual de CO_2 entre el suelo y la atmósfera puede presentar una gran magnitud y gran variabilidad espacio-temporal, de manera que resulta clave tener un conocimiento claro de los factores que controlan la dinámica del C en el suelo. Con respecto al C orgánico del suelo (COS), los factores climáticos han sido considerado por muchos investigadores (Davidson, 2015; Carvalhai et al. 2014; Craine et al. 2010; Davidson & Jensssen, 2006), como los principales componentes que determinan la descomposición de la materia orgánica (MO) y la liberación de CO_2. No obstante, actualmente se ha encontrado que la geoquímica del suelo y su interacción con el clima puede tener un rol en el control de la acumulación de C en el suelo (Van der Voort et al. 2016; Xu et al. 2016; Doetterl et al. 2015). Para cuantificar el efecto de la geoquímica del suelo es importante conocer la composición del material parental del suelo y su estado de meteorización, todo lo cual resulta importante para explicar su interacción con el clima, en los mecanismos de estabilización

del C, ayudando a mejorar los modelos globales terrestres (global earth models) existentes y el poder predictivo de estos en relación a la contribución del COS al fenómeno de cambio climático.

1.2 Mecanismos de estabilización de la materia orgánica en el suelo.

Los mecanismos de estabilización y/o descomposición de la MO han sido ampliamente estudiados (Conant et al. 2011; Lützow et al. 2006; Six et al. 2002), especialmente en los horizontes superficiales del perfil de suelo, donde los mecanismos físicos y químicos de estabilización combinan procesos de adsorción sobre superficies minerales o componentes inorgánicos del suelo como hidróxidos amorfos de aluminio (Al) y hierro (Fe), arcillas o arcillas coloidales, tales como alofán en Andisoles (Matus et al. 2008). La protección física de la MO incluye, por ejemplo, la formación de agregados que impiden la descomposición de la MO atrapada en su interior. Sin embargo, no se conoce bien la dinámica de estabilización y descomposición del C en los horizontes más profundos de un perfil de suelo y en diferentes condiciones medioambientales. Por lo tanto, se necesitan más conocimientos para comprender mejor la dinámica potencial del C a escala global y en profundidad, por ejemplo, estudiando gradientes latitudinales a través de una serie de tipos de suelo y entornos ambientales. Es aquí donde las técnicas que usan isótopos estables como ^{13}C se han transformados en herramientas útiles para entender la dinámica del COS en el subsuelo (Mathieu et al. 2015; Acton et al. 2013; Chen et al. 2005).

1.3 Dinámica del carbono del suelo y su relación con isótopos de carbono estables.

El análisis de la abundancia natural de ^{13}C es una técnica ampliamente utilizada y probada en el estudio de la descomposición de la MO del suelo y del ciclo del C (Accoe et al. 2003; Ehleringer et al. 2002). Este método relativamente nuevo ha sido utilizado para evaluar la dinámica del C en la cuantificación de las variaciones en la relación $^{13}C/^{12}C$ del COS a diferentes profundidades en el perfil del suelo (Accoe et al. 2003; Ågren et al. 1996; Bird et al. 1997; Feng, 2002; Jones et al. 2009; Poago & Feng, 2004; Powers et al. 2002; Wang et al. 2017). La composición de isótopos estables de C y su abundancia natural ha demostrado ser útil para examinar, entre otros, los procesos ecológicos y biogeoquímicos relacionados con los ecosistemas; proporcionando información a escala temporal y espacial sobre la estabilización y descomposición del C (Poage, 2004; Tcherkz et al. 2011). Los isótopos de C estables son expresados como $\delta^{13}C$ en tanto por mil (‰) relativo a V-PDB (Vienna Pee Dee Belemnite), donde los valores correspondientes a la MO del suelo son determinados por los valores de $\delta^{13}C$ del material vegetal del cual deriven (plantas tipo C3 o C4). Los cambios en vegetación desde plantas C3 a C4 han sido utilizados para cuantificar procesos de descomposición de la MO, basados en el aumento gradual de los valores de $\delta^{13}C$ en el suelo derivados desde el $\delta^{13}C$ de plantas C3 a $\delta^{13}C$ de plantas C4, asumiendo que la diferencia en los valores de $\delta^{13}C$ no cambia durante los procesos de descomposición. Por otra parte, existen otros factores que determinan la acumulación de estos isótopos en el suelo de lo cual se desprende una segunda premisa, la cual establece que los valores de $\delta^{13}C$

de la MO del suelo incrementan en un 1 - 3 ‰ con la profundidad, debido a uno o más de los siguientes procesos: 1) descomposición microbiana (fraccionamiento del ^{13}C por microorganismos del suelo durante la descomposición de la MO y adición de ^{13}C enriquecido por la biomasa microbiana), 2) efecto de Suess (agotamiento del ^{13}C del C atmosférico desde la industrialización) y 3) La protección física y química del material polisacárido de los aportes de materia orgánica de hojas y raíces que muestra una amplia gama de valores isotópicos (Brugnoli & Farquhar, 2000; Tcherkez et al. 2011). Un perfil vertical de $\delta^{13}C$ podría ser usado entonces como un indicador de la tasa de descomposición del COS (Acton et al. 2013; Campbell et al. 2009). Accoe et al. (2003) reportaron que la constante de la tasa de descomposición en muestras de 0 a 40 cm de profundidad (en intervalos de 0-10, 10-20, 20,-30 y 30-40 cm), tomadas de distintos sitios de pastizales, exhibió una correlación significativa y positiva entre los correspondientes valores de $\Delta\delta^{13}C$ (cambio del valor $\delta^{13}C$ por incremento de profundidad). Otros autores han reportado aumentos en los valores de $\delta^{13}C$ a medida que disminuye la concentración de COS, al aumentar en profundidad del perfil analizado (Acton et al. 2013; Garten and Hansen, 2006). Ya que la pendiente del ajuste lineal entre $\delta^{13}C$ del suelo y el log del COS refleja la tasa de descomposición de este, indica que un aumento en la concentración del isótopo se encuentra relacionado con una disminución en la tasa de descomposición de la MO del suelo. Por otra parte, se necesitan más conocimientos para comprender mejor la dinámica potencial del C a escala global, por ejemplo, estudiando transectos latitudinales a través de una serie de tipos de suelo y entornos ambientales. Sin embargo, esto exige

que se analice un elevado número de muestras de suelo, lo que puede llevar mucho tiempo y ser costoso utilizando los métodos convencionales para la determinación del $\delta^{13}C$ del suelo (es decir, análisis elemental - espectrometría de masas de relación isotópica, EA-IRMS). El uso de la espectroscopia de reflectancia difusa infrarroja en el rango espectral del infrarrojo cercano (NIRS) (Fuentes et al. 2012; Sepúlveda et al. 2021; Winowiecki et al. 2017) podría proporcionar una alternativa rentable y rápida a los métodos tradicionales para evaluar el $\delta^{13}C$ del suelo.

1.4 Técnica NIRS (Espectroscopia Infra-Rojo Cercano) y su uso en predicciones de isótopos de carbono estables.

La aplicación de NIRS en propiedades del suelo, mineralización de COS, funciones microbianas y clasificaciones de la condición del suelo han sido ampliamente reportada en la literatura (Awiti et al. 2008; Schimann et al. 2007; Mutuo et al. 2006; Viscarra Rossel et al. 2006; Chang et al. 2001); sin embargo, existen menos reportes de esta técnica en la predicción de isótopos estables en suelo, a pesar del hecho que otros estudios en tejido vegetal han mostrado la pertinencia de esta técnica para predecir $\delta^{13}C$ y $\delta^{15}N$ (Clark et al. 1995; Kleinebecker et al. 2009). Fuentes et al. (2009, 2012) aplican la técnica NIRS para predecir tanto C estable como también isótopos de N para una determinada zona agrícola de México, analizando tratamientos combinados con retención de residuos en el cultivo (N=50; $\delta^{13}C$ $^{0}/_{00}$ desde -16.6 a -23.3) y suelos sin retención de residuos en el cultivo (N=50; $\delta^{13}C$ $^{0}/_{00}$ desde -19.1 a -22.1). Este autor utilizó un análisis estadístico de regresión de mínimos cuadrados

parciales modificado para desarrollar diferentes modelos de calibración consiguiendo un R^2 de 0.81. A pesar de que sus resultados demuestran el potencial de la técnica, la debilidad de la investigación fue el uso de un solo suelo, tampoco incorporó la influencia o variación de las características químicas y físicas del suelo en el modelo. Así el potencial real y pertinencia de la técnica de NIRS prediciendo el ^{13}C en suelo debiese ser probado considerando una mayor cantidad de sitios de estudio, con distintos tipos de suelo y clima. Utilizando gradientes naturales (Brunn et al. 2016; Doetterl et al. 2015). En este aspecto, Chile presenta una geomorfología de más de 4000 Km de largo, ideal para estudios de gradientes latitudinales debido a su diversidad edafo-climática. Así como también, en el análisis de patrones verticales de contenido de ^{13}C de la MO (Brunn et al., 2016), cuando se pretende estudiar la dinámica del CO en el sub-suelo, se recomienda asegurar una variabilidad en las propiedades químicas y físicas del suelo con una mayor cantidad de muestras (Winowiecki et al. 2017).

Con la creciente disponibilidad de datos de $\delta^{13}C$ de SOM, éstos se están utilizando más ampliamente para evaluar la dinámica del C, comprender las tasas de rotación del C del suelo y los procesos que afectan a la (des)estabilización del C del suelo para la implementación de modelos (Acton et al. 2013; Poage & Feng, 2004; Wang et al. 2018; Wynn et al. 2005). Los procesos climáticos y biogeoquímicos pueden jugar un papel clave en la formación y persistencia de SOM (Davidson, 2015), impactando en el $\delta^{13}C$ (Arora et al. 2013; Robertson et al. 2019). Con lo que, podría obtenerse información crucial a partir de la comprensión del agotamiento y el

enriquecimiento de $\delta^{13}C$ en el suelo y ayudar a predecir procesos de estabilización/desestabilización del C, que son relevantes en el contexto de las predicciones del efecto de un cambio climático mayor (Bird et al. 1997; Powers et al. 2002; Ramírez et al. 2020).

2. HIPÓTESIS

El contenido del C estable (^{13}C) estimado a través de espectrometría del espectro infrarrojo cercano (NIRS) estima los cambios en $\delta^{13}C$ en el perfil del suelo ($\Delta\delta^{13}C$) y su relación con las tasas de mineralización del C y potencial especifico de respiración en diferentes escenarios edafoclimáticos. La comprobación de esta inferencia conformará un indicador de la degradabilidad de la MO del suelo, y de la influencia de los factores geoquímicos y climáticos en el poder predictivo de la señal isotópica.

3. OBJETIVO GENERAL

- Determinar los cambios en ($\Delta\delta^{13}C$) a diferentes profundidades en el perfil del suelo a través del uso de una técnica NIRS y estudiar su relación con las correspondientes tasas de descomposición para predecir la degradabilidad del C del suelo en un gradiente edafoclimático de Chile.

4. OBJETIVOS ESPECÍFICOS

- Determinar la evolución del contenido de C y la abundancia natural del ^{13}C (valor $\delta^{13}C$) en el perfil del suelo para estudiar la interacción entre el clima y las propiedades geoquímicas del suelo sobre la dinámica del C orgánico en perfiles de suelos minerales.

- Determinar las tasas de mineralización de C y potencial específico de respiración a distintas profundidades del perfil del suelo

- Identificar los principales factores geoquímicos que influyen en la abundancia del $\delta^{13}C$ y sus cambios en el perfil del suelo.

- Relacionar esta dinámica del C (tasa de mineralización del COS y el potencial específico de respiración del suelo) a distintas profundidades del perfil con la señal isotópica del $\Delta\delta^{13}C$.

LITERATURA CITADA

Accoe, F., Boeckx, P., Cleemput, O. V., & Hofman, G. (2003). Relationship between soil organic C degradability and the evolution of the $\delta^{13}C$ signature in profiles under permanent grassland. Rapid Communications in Mass Spectrometry, 17(23), 2591-2596.

Acton, P., Fox, J., Campbell, E., Rowe, H., & Wilkinson, M. (2013). Carbon isotopes for estimating soil decomposition and physical mixing in well-drained forest soils. Journal of Geophysical Research: Biogeosciences, 118(4), 1532-1545.

Ågren, G. I., E. Bosatta, and J. Balesdent, Isotope discrimination during decomposition of organic matter: A theoretical analysis, Soil Sci. Soc. Am.

J., 60, 1121– 1126, 1996.

Arora, V. K., Boer, G. J., Friedlingstein, P., Eby, M., Jones, C. D., Christian, J. R., ... & Wu, T. (2013). Carbon–concentration and carbon-climate feedbacks in CMIP5 Earth system models. Journal of Climate, 26(15), 5289-5314.

Awiti, A. O., Walsh, M. G., Shepherd, K. D., & Kinyamario, J. (2008). Soil condition classification using infrared spectroscopy: A proposition for assessment of soil condition along a tropical forest-cropland chronosequence. Geoderma, 143(1), 73-84.

Bird, M. I., & Pousai, P. (1997). Variations of $\delta^{13}C$ in the surface soil organic carbon pool. Global Biogeochemical Cycles, 11(3), 313-322.

Brugnoli, E., & Farquhar, G. D. (2000). Photosynthetic fractionation of carbon isotopes. In Photosynthesis (pp. 399-434). Springer, Dordrecht.

Brunn, M., Condron, L., Wells, A., Spielvogel, S., & Oelmann, Y. (2016). Vertical distribution of carbon and nitrogen stable isotope ratios in topsoils across a temperate rainforest dune chronosequence in New Zealand. Biogeochemistry, 129(1-2), 37-51.

Campbell, J. E., Fox, J. F., Davis, C. M., Rowe, H. D., & Thompson, N. (2009). Carbon and nitrogen isotopic measurements from southern Appalachian soils: Assessing soil carbon sequestration under climate and land-use variation. Journal of Environmental Engineering, 135(6), 439-448.

Carvalhais, N., Forkel, M., Khomik, M., Bellarby, J., Jung, M., Migliavacca, M., & Weber, U. (2014). Global covariation of carbon turnover times with climate in terrestrial ecosystems. Nature, 514(7521), 213.

Chang, C. W., Laird, D. A., Mausbach, M. J., & Hurburgh, C. R. (2001). Near-infrared reflectance spectroscopy–principal components regression analyses of soil properties. Soil Science Society of America Journal, 65(2), 480-490.

Chen, Q., Shen, C., Sun, Y., Peng, S., Yi, W., Li, Z. A., & Jiang, M. (2005). Spatial and temporal distribution of carbon isotopes in soil organic matter at the Dinghushan Biosphere Reserve, South China. Plant and Soil, 273(1-2),

115-128.

Clark, D. H., Johnson, D. A., Kephart, K. D., & Jackson, N. A. (1995). Near infrared reflectance spectroscopy estimation of ^{13}C discrimination in forages. Journal of Range Management, XX, 132-136.

Conant, R. T., Ryan, M. G., Ågren, G. I., Birge, H. E., Davidson, E. A., Eliasson, P. E., ... & Hyvönen, R. (2011). Temperature and soil organic matter decomposition rates–synthesis of current knowledge and a way forward. Global Change Biology, 17(11), 3392-3404.

Craine, J. M., Fierer, N., & McLauchlan, K. K. (2010). Widespread coupling between the rate and temperature sensitivity of organic matter decay. Nature Geoscience, 3(12), 854.

Davidson, E. A., & Janssens, I. A. (2006). Temperature sensitivity of soil carbon decomposition and feedbacks to climate change. Nature, 440(7081), 165-173.

Davidson, E. A. (2015). Biogeochemistry: soil carbon in a beer can. Nature Geoscience, 8(10), 748.

Doetterl, S., Cornelis, J. T., Six, J., Bodé, S., Opfergelt, S., Boeckx, P., & Van Oost, K. (2015). Soil redistribution and weathering controlling the fate of geochemical and physical carbon stabilization mechanisms in soils of an eroding landscape. Biogeosciences, 12(5), 1357-1371.

Ehleringer, J. R., Bowling, D. R., Flanagan, L. B., Fessenden, J., Helliker, B., Martinelli, L. A., & Ometto, J. P. (2002). Stable isotopes and carbon cycle processes in forests and grasslands. Plant Biology, 4(2), 181-189.

Feng, X. (2002). A theoretical analysis of carbon isotope evolution of decomposing plant litters and soil organic matter. Global Biogeochemical Cycles, 16(4), 66-1.

Fuentes, M., González-Martín, I., Hernández-Hierro, J. M., Hidalgo, C., Govaerts, B., Etchevers, J., & Dendooven, L. (2009). The natural abundance of ^{13}C with different agricultural management by NIRS with fibre optic probe technology. Talanta, 79(1), 32-37.

Fuentes, M., Hidalgo, C., González-Martín, I., Hernández-Hierro, J. M., Govaerts, B., Sayre, K. D., & Etchevers, J. (2012). NIR spectroscopy: An alternative for soil analysis. Communications in Soil Science and Plant Analysis, 43(1-2), 346-356.

Garten, C. T., & Hansen, P. J. (2006). Measured forest soil C stocks and estimated turnover times along an elevation gradient. Geoderma, 136(1), 342-352.

IPCC. 2013. Climate change 2013: The physical science basis. Summary for policymakers. Contribution of working group I to the fourth assessment report of the Intergovernmental Panel on Climate Change (IPCC). p. 1-18. In: S. Solomon et al. (eds.) Cambridge University Press, Cambridge, UK.

Jones,D. L., Kielland, K., Sinclair, F. L., Dahlgren, R. A., Newsham, K. K., Farrar, J. F., & Murphy, D. V. (2009). Soil organic nitrogen mineralization across a global latitudinal gradient. Global Biogeochemical Cycles, 23(1).

Kleinebecker, T., Schmidt, S. R., Fritz, C., Smolders, A. J., & Hölzel, N. (2009). Prediction of $\delta^{13}C$ and $\delta 15N$ in plant tissues with near-infrared reflectance spectroscopy. New Phytologist, 184(3), 732-739.

Lal, R. 2006. Soil carbon sequestration in Latin America. p. 49-64. In Lal, R. et al. (eds.) Carbon sequestration in soils of Latin America. The Haworth Press, Binghamton, New York, USA.

Mathieu, J. A., Hatté, C., Balesdent, J., & Parent, É. (2015). Deep soil carbon dynamics are driven more by soil type than by climate: a worldwide meta-analysis of radiocarbon profiles. Global Change Biology. DOI: 10.1111/gcb.13012

Matus, F., Garrido, E., Sepúlveda, N., Cárcamo, I., Panichini, M., & Zagal, E. (2008). Relationship between extractable Al and organic C in volcanic soils of Chile. Geoderma, 148(2), 180-188

Mutuo, P. K., Shepherd, K. D., Albrecht, A., & Cadisch, G. (2006). Prediction of carbon mineralization rates from different soil physical fractions using diffuse

reflectance spectroscopy. Soil Biology and Biochemistry, 38(7), 1658-1664.

Lützow, M. V., Kögel-Knabner, I., Ekschmitt, K., Matzner, E., Guggenberger, G., Marschner, B., & Flessa, H. (2006). Stabilization of organic matter in temperate soils: mechanisms and their relevance under different soil conditions–a review. European Journal of Soil Science, 57(4), 426-445.

Poage, M. A., & Feng, X. (2004). A theoretical analysis of steady state $\delta^{13}C$ profiles of soil organic matter. Global biogeochemical cycles, 18(2).

Powers, J. S., & Schlesinger, W. H. (2002). Geographic and vertical patterns of stable carbon isotopes in tropical rain forest soils of Costa Rica. Geoderma, 109(1-2), 141-160.

Powlson, D., Smith, P., Nobili, M.D. (2012). Soil organic matter. pp. 87 - 131 Gregory, P. J., & Nortcliff, S. (Eds.). Soil conditions and plant growth. John Wiley & Sons.

Ramírez, P. B., Calderón, F. J., Fonte, S. J., Santibáñez, F., & Bonilla, C. A. (2020). Spectral responses to labile organic carbon fractions as useful soil quality indicators across a climatic gradient. Ecological Indicators, 111, 106042.

Reay, D., and J. Grace. 2007. Carbon dioxide: Importance, sources and sinks. p. 1-10. In D. Reay et al. (eds.) Greenhouse gas sinks. CAB International, Wallingford, UK.

Robertson, A. D., Paustian, K., Ogle, S., Wallenstein, M. D., Lugato, E., & Cotrufo, M. F. (2019). Unifying soil organic matter formation and persistence frameworks: the MEMS model. Biogeosciences, 16(6), 1225-1248.

Rossel, R. V., Walvoort, D. J. J., McBratney, A. B., Janik, L. J., & Skjemstad, J. O. (2006). Visible, near infrared, mid infrared or combined diffuse reflectance spectroscopy for simultaneous assessment of various soil properties. Geoderma, 131(1-2), 59-75.

Sadzawka, A., Carrasco, M., Grez, R., Mora, M., & Flores, H. y A. Neaman.

2006. Métodos de análisis recomendados para los suelos de Chile. Serie Actas INIA, (34), 164.

Schimann, H., Joffre, R., Roggy, J. C., Lensi, R., & Domenach, A. M. (2007). Evaluation of the recovery of microbial functions during soil restoration using near-infrared spectroscopy. Applied Soil Ecology, 37(3), 223-232.

de los Ángeles Sepúlveda, M., Hidalgo, M., Araya, J., Casanova, M., Muñoz, C., Doetterl, S., ... & Zagal, E. (2021). Near-infrared spectroscopy: Alternative method for assessment of stable carbon isotopes in various soil profiles in Chile. Geoderma Regional, 25, e00397.

Shepherd, K. D., Vanlauwe, B., Gachengo, C. N., & Palm, C. A. (2005). Decomposition and mineralization of organic residues predicted using near infrared spectroscopy. Plant and Soil, 277(1-2), 315-333.

Six, J., Conant, R. T., Paul, E. A., & Paustian, K. (2002). Stabilization mechanisms of soil organic matter: implications for C-saturation of soils. Plant and soil, 241(2), 155-176.

Tcherkez, G., Mahé, A., & Hodges, M. (2011). $^{12}C/^{13}C$ fractionations in plant primary metabolism. Trends in plant science, 16(9), 499-506.

Team, R. C. (2014). A language and environment for statistical computing. R Foundation for Statistical Computing, Vienna.

Torn, M. S., Trumbore, S. E., Chadwick, O. A., Vitousek, P. M., & Hendricks, D. M. (1997). Mineral control of soil organic carbon storage and turnover. Nature, 389(6647), 170-173.

Van der Voort, T. S., Hagedorn, F., McIntyre, C., Zell, C., Walthert, L., Schleppi, P., & Eglinton, T. I. (2016). Variability in 14 C contents of soil organic matter at the plot and regional scale across climatic and geologic gradients. Biogeosciences, 13(11), 3427.

Wang, C., Wei, H., Liu, D., Luo, W., Hou, J., Cheng, W., ... & Bai, E. (2017). Depth profiles of soil carbon isotopes along a semi-arid grassland transect in northern China. Plant and Soil, 417(1), 43-52.

Wang, C., Houlton, B. Z., Liu, D., Hou, J., Cheng, W., & Bai, E. (2018). Stable isotopic constraints on global soil organic carbon turnover. Biogeosciences, 15(4), 987-995.

Winowiecki, L. A., Vågen, T. G., Boeckx, P., & Dungait, J. A. (2017). Landscape-scale assessments of stable carbon isotopes in soil under diverse vegetation classes in East Africa: application of near-infrared spectroscopy. Plant and Soil, 421(1-2), 259-272.

Wynn, J. G., Bird, M. I., & Wong, V. N. (2005). Rayleigh distillation and the depth profile of $^{12}C/^{13}C$ ratios of soil organic carbon from soils of disparate texture in Iron Range National Park, Far North Queensland, Australia. Geochimica et cosmochimica acta, 69(8), 1961-1973.

Xu, X., Shi, Z., Li, D., Rey, A., Ruan, H., Craine, J. M., ... & Luo, Y. (2016). Soil properties control decomposition of soil organic carbon: Results from data-assimilation analysis. Geoderma, 262, 235-242.

II. CAPITULO 2.

NEAR-INFRARED SPECTROSCOPY: ALTERNATIVE METHOD FOR ASSESSMENT OF STABLE CARBON ISOTOPES IN VARIOUS SOIL PROFILES IN CHILE

María de los Angeles Sepulveda[1], Marcela Hidalgo[1], Juan Araya[2], Manuel Casanova[3], Cristina Muñoz[1], Sebastian Doetterl[4], Daniel Wasner[4], Ben Colpaert[5], Samuel Bodé[5], Pascal Boeckx[5], Erick Zagal[1]*

[1] Department of Soil and Natural Resources, Faculty of Agronomy, University of Concepción, Chile
[2] Department of Instrumental Analysis, Faculty of Pharmacy, University of Concepción, Chile
[3] Department of Engineering and Soil, Faculty of Agronomics Science, University of Chile, Santiago, Chile
[4] ETH-Zürich, Department of Environmental Systems Science, Zürich, Switzerland
[5] Department of Green Chemistry and Technology, Isotope Bioscience Laboratory (ISOFYS), Ghent University, Gent, Belgium
* Corresponding author: ezagal@udec.cl; Vicente Méndez 595, Chillán, Chile

Artículo publicado en Geoderma Regional, Volume 25, June 2021, e00397

Abstract

The role of soil in the global carbon cycle and carbon–climate feedback mechanisms has attracted considerable interest in recent decades. Consequently, development of simple, rapid, and inexpensive methods to support the studies on carbon dynamics in soil is of interest. Near-infrared spectroscopy (NIRS) has emerged as a rapid and cost-effective method for measurements of soil properties. The aim of this study was to develop and validate a predictive model for $\delta^{13}C$ values using NIRS in various soil profiles across Chile. Eleven sites were selected in the range of 30° to 50° S. These sites represent different soil moisture and soil temperature regimes, clay mineralogies, parent materials, and climates; in addition, they have prairie vegetations and contain C3-type vegetations. Air-dried soil samples were scanned in the NIR range at a resolution of 4 cm^{-1}. The carbon isotopic composition, expressed as $\delta^{13}C$ relative to the Vienna Pee Dee Belemnite standard, was analysed using an elemental analyser–isotope ratio mass spectrometer system. A prediction model for $\delta^{13}C$ values based on NIRS data was developed through a partial least-squares regression (PLS) model using ten latent variables. A second model was generated using a random forest (RF) approach. The model performances were acceptable. The RF model provided the best results. The values of the root mean square error of prediction for the validation runs for $\delta^{13}C$ obtained using the PLS and RF models were 1.41% and 1.15%, respectively. These model performances indicate that NIRS can be used to predict $\delta^{13}C$ for the selected dataset. The results of this study support the use

of NIRS as a predictive method in soil analyses and as a nondestructive waste-free method for studies on carbon dynamics in soil.

Keywords: Near-infrared spectroscopy, Isotope ratio mass spectrometer, Carbon isotope abundance, $\delta^{13}C$, Andisols, Alfisols, Inceptisols, Mollisols, Carbon dynamics, Partial least-squares regression

1. INTRODUCTION

Soil organic carbon (SOC) is one of the largest reserves of carbon in terrestrial ecosystems (Lal, 2006). However, studies indicate that the exchange of SOC with the atmosphere can vary depending on climatic conditions, which leads to questions whether the soil is a source or sink for atmospheric carbon dioxide (CO_2) (Carvalhais et al., 2014). Therefore, the understanding of SOC dynamics, particularly the carbon stabilisation, is crucial to predict the role of SOC in the carbon cycle under a changing climate (Crowther et al., 2016). The potential of soil to sequester carbon depends primarily on the soil development and interactions between weathering and biological processes that affect the nutrient availability (Doetterl et al., 2018).

Climatic factors control the SOC degradation (Carvalhais et al., 2014), while geochemical factors stabilise soil organic matter (SOM). The interaction between climatic and geochemical factors in soil carbon storage has attracted attention (Doetterl et al., 2015). Furthermore, the climate, vegetation, and geochemical soil composition affect the SOC dynamics (Finke et al., 2019). The

influence of the parent material on the soil geochemistry reveals the importance of the paedological characteristics and soil types as factors of stabilising influences on the SOC (Finke et al., 2019).

An intensive and reliable mapping is required to monitor changes in soil organic pools (Bricklemyer et al., 2005; Mooney et al., 2004), as well as small scale studies. The SOM composition and carbon dynamics have been studied in topsoil horizons for a long time. Over the past decade, subsoil horizons have been actively investigated because the subsoil carbon contributes to the total carbon stocks. The understanding of the factors that stabilise carbon in deeper soil layers is still limited, which is essential to understand the feedback mechanisms between SOC stocks and atmospheric CO_2 during climate changes (Chabbi et al., 2009; Rumpel et al., 2002; Fontaine et al., 2007). Accurate and low-cost methods of soil analysis are required because the number of soil samples typically involved in such studies is large. During the past two decades, visible–near-infrared (vis–NIR) diffuse reflectance spectroscopy has been developed as an easy-to-use method, suitable for prediction of several soil properties (e.g., % C, % N, pH, and texture) (Viscarra Rossel et al., 2006; Petisco et al., 2006; Zornoza et al., 2008).

Numerous methods can be used to study the dynamics of SOC. Techniques that can measure the isotopic abundance of ^{13}C in SOC are useful to elucidate C-process dynamics (Balesdent et al., 1993; Balesdent and Mariotti, 1996; Glaser, 2005; Trumbore, 2009; Accoe et al., 2003). Accoe et al. (2003) proposed that the change in ^{13}C content in soil profiles can be used as an indicator of the stability of SOM. The isotopic ratios of several elements (e.g., carbon, nitrogen,

and oxygen) in the soil are typically determined using isotope ratio mass spectrometry (IRMS) (Balesdent and Mariotti, 1996; Glaser, 2005; Trumbore, 2009). However, IRMS is complex and requires both sophisticated equipment and trained personnel, which limits the number of samples that can be analysed. Near-infrared reflectance spectroscopy (NIRS) has numerous characteristics of interest for agronomic and environmental studies. The sample preparation involves only drying and grinding. The analysis is nondestructive, without hazardous chemicals. In addition, the measurement period is only a few seconds. Furthermore, NIRS is suitable for analyses of large samples. Multiple soil properties can be estimated by a single scan. In recent years, NIRS has also been used to determine the abundance of stable carbon isotopes in soil. NIRS has been used to predict $\delta^{13}C$ in soil (Fuentes et al., 2012; Winowiecki et al., 2017). These studies indicate that infrared spectroscopy is a promising method to estimate $\delta^{13}C$ in soil, which can enable an increased number of analysed samples, often required for studies on carbon dynamics in soil (Accoe et al., 2003).

NIRS generates complex absorption patterns, which need to be mathematically processed to correlate latent variables with soil properties (Stenberg et al., 2010). Such analyses of soil spectra require multi-variate calibrations (Martens and Naes, 1989) to capture the information relevant to the calibration and validation of predictive models. Recently, the number of studies on the multi-variate analysis of NIRS data has largely increased. Good results have been obtained for multiple soil properties (Theo, 2005; Viscarra Rossel et al., 2006;

Viscarra Rossel and McBratney, 1998; Zornoza et al., 2008). NIRS is a more accessible method for the analysis and a more suitable alternative to conventional chemical methods of soil analysis (Fuentes et al., 2012).

We report the development and validation of a predictive model to estimate $\delta^{13}C$ in topsoil and subsoils, which can improve our knowledge of the mechanisms of SOC stocks during climate changes. In contrast to those in other studies, this model attributed the changes in the signals to various soil types and profiles under different climatic conditions. The implementation of this alternative methodology using NIRS to assess stable isotopes of carbon in soil is presented as a viable and low-cost technique for studies on soil carbon dynamics in wide transects and at different depths, which are factors that increase the complexity and cost of the analysis.

2. MATERIALS AND METHODS

2.1. Soil sampling

From the Chilean Coquimbo Region to the Magallanes Region (30°–50° S), a total of eleven sites were carefully chosen to represent the soil transect (see Doetterl et al. (2015) for the used selection criteria). The criteria included soils with a broad pH range (4.6–7.5) and null HCl reaction, soils having various soil moisture regimes (SMRs) (aridic, ustic, xeric, udic, and perudic), soil temperature regimes (STRs) (thermic, isothermic, mesic, isomesic, and cryic), and clay mineralogies (short range order mineral phases and crystalline), soils with different parent materials (volcanic ash, alluvial, fluvio-glacial material,

marine sediment, etc.), soils located within different climatic zones (arid–semiarid, Mediterranean arid, Mediterranean humid, humid, and Magallanian), and soils under natural prairie vegetation conditions (C3-type vegetation). Field sampling campaigns were carried out primarily during summer (2017–2018). Sampling units were defined in plots of 50 × 50 m, from which six random soil cores were extracted. These campaigns were an extension of the transect reported by Doetterl et al. (2015) and included additional depths of soil layers. Some of the new sites used in this study are listed in Tables 1 and 2. We selected eleven sites for this study from the sites sampled in the previous transect (Doetterl et al., 2015) and extension campaign. We chose these sites to maximise the climatic and physicochemical diversities of the soils to train models with the widest range of application. Site locations and basic physicochemical variables are listed in Tables 1 and 2 (Figure 1).

2.2. Sample preparation

Soil samples were collected in triplicate to a depth of 30 cm or 60 cm (until gravel material was encountered) using polyvinylchloride (PVC) tubes (height: 35 cm; diameter: 90 mm) to extract undisturbed soil samples. The samples were then transported to the University of Concepción, where they were stored at −20 °C until further processing. Soil sample profiles were obtained at intervals of 2 cm to a depth of 10 cm, at intervals of 5 cm in the depth range of 10-30 cm, and at intervals of 10 cm in the depth range of 30-60 cm. To obtain detailed soil layer data, the tubes were cut using a custom-designed device, which actioned a steel saw unit at a high speed. The procedures were carried out very carefully to

avoid contamination of the soil with PVC powder or other materials. The samples were air-dried and sieved at 2 mm. The fine roots were removed using electrostatic energy, as described by Kuzyakov et al. (2001).

Table 1. Description of the 11 sites used for the calibration and validation of the predictive model.

Soil series	WGS1984 X (ddd,ddd)	WGS1984 Y (ddd,ddd)	STR	SMR	Soil suborder (Soil taxonomy)	Geomorphology
Calle Larga	-70.52162	-32.87609	Thermic	Xeric	Typic Argixeroll	Piedmont
Pimpinela	-70.72972	-34.32387	Thermic	Xeric	Mollic Haploxeralf	Piedmont
Bramaderos	-71.31464	-35.61330	Thermic	Xeric	Humic Haploxerand	High alluvial terraces
Santa Bárbara	-71.69721	-36.45816	Thermic	Xeric	Typic Haploxerand	Old fluvio-glacial terraces
Choshuenco	-72.11120	-39.85941	Isomesic	Udic	Andic Dystrudept	Hillocks and hills
Mayamó	-73.79915	-42.05300	Isomesic	Perudic	Acrudoxic Durudand	Gentle rolling hills
Aituí	-73.61712	-43.05791	Isomesic	Perudic	Hydric Fulvudand	High planes
Puerto Cisnes	-72.61337	-45.38105	Isomesic	Perudic	Acrudoxic Fulvudand	Fluvio-glacial terrace
Bahía Exploradores	-73.06868	-46.50487	Mesic	Udic	Oxyaquic Hapludand	Hills
Aguas Frescas	-70.98.860	-53.43267	Cryic	Udic	Inceptisol	Marine terraces
Santa Olga	-70.36106	-53.31478	Isomesic	Perudic	Inceptisol	Marine terraces

X and Y: coordinates; STR: soil thermic regime; SMR: soil moisture regime.

Table 2. Chemical and physical properties of the 11 sites used for the model construction.

Soil series / Depth (cm)	Nitrogen (g N • kg^{-1} soil)			Carbon (g C • kg^{-1} soil)			Bulk density (gr • cm^{-3})			pH (KCl)			TRB (cmol$_c$ • kg^{-1})			Clay %		
	0-10	10-30	30-60	0-10	10-30	30-60	0-10	10-30	30-60	0-10	10-30	30-60	0-10	10-30	30-60	0-10	10-30	30-60
Calle Larga	5.8	2.3	ns	52.2	20.9	ns	1.4	1.8	ns	5.3	5.3	ns	23.8	19.9	ns	32.3	32.7	ns
Pimpinela	2.0	1.6	ns	20.1	14.6	ns	0.9	1.1	ns	5.5	5.5	ns	13.4	17.0	ns	36.0	37.1	ns
Bramaderos	4.7	5.1	4.4	54.5	59.8	55.4	1.4	1.5	0.9	5.1	5.1	5.1	10.5	10.1	8.8	20.7	26.1	19.9
Santa Bárbara	5.1	3.3	2.1	62.4	40.6	23.8	0.8	0.7	0.6	4.9	5.3	5.8	2.1	5.4	5.8	29.5	37.8	35.5
Choshuenco	9.3	4.3	3.9	108.0	43.3	47.1	0.7	0.5	0.8	4.5	4.8	5.1	3.5	1.9	3.7	15.6	7.2	10.7
Mayamó	11.0	6.4	4.6	138.6	91.9	59.4	0.7	0.6	0.8	4.4	4.3	5.1	4.6	1.9	0.7	8.4	15.6	23.9
Aituí	13.7	7.5	5.4	171.9	105.2	71.1	0.6	0.4	0.5	4.6	4.7	5.2	5.3	1.9	1.0	16.8	19.2	31.6
Puerto Cisnes	16.1	10.4	6.6	163.9	126.5	82.8	0.5	0.6	0.3	4.2	4.7	4.6	2.7	1.1	2.1	17.5	10.4	21.8
Bahía Exploradores	4.9	1.0	1.0	60.7	15.8	14.5	1.7	1.7	1.0	4.0	4.7	4.4	2.1	0.3	0.5	24.3	25.5	22.0
Aguas Frescas	4.5	0.5	ns	67.7	13.3	ns	0.7	0.7	ns	4.8	4.3	ns	27.3	1.8	ns	7.6	9.9	ns
Santa Olga	7.7	4.8	ns	150.2	91.9	ns	0.6	0.8	ns	4.0	3.9	ns	12.9	9.5	ns	13.0	23.1	ns

ns: not sampled owing to excess of gravel

2.3. Laboratory analysis

The samples were air-dried and scanned at NIR wavelengths (800–2857 nm) by diffuse reflectance spectroscopy. The resolution was 4 cm^{-1}. The Fourier-transform NIR system was a Bruker Matrix-I (Bruker Optics, Rheinstetten, Germany) located at the Soil and Environmental Laboratory of the Department of Soil and Natural Resources, Faculty of Agronomy, Universidad de Concepción. The total carbon contents (% C), total nitrogen contents (% N), and isotopic ratios ($^{13}C/^{12}C$) of 332 samples were determined using an elemental analysis (EA)–IRMS (ANCA-SL, Sercon, Crewe, UK) system, coupled to a 2020 IRMS system (Sercon, Crewe, UK), at the Isotope Bioscience Laboratory (ISOFYS, www.isofys.be) of Ghent University, Belgium. The carbon isotopic ratio ($^{13}C/^{12}C$) of the soil sample is expressed relative to an international reference, using the delta notation ($\delta^{13}C$). The delta value expresses the fractional difference in the isotopic ratio between the sample and international reference. For ^{13}C, the used international reference standard was Vienna Pee Dee Belemnite (VPDB), typically expressed in parts per thousand (‰) (Chen et al., 2005).

For soil chemical and physical analyses (three composite samples per site, at 0–10 cm, 10–30 cm, and (where applicable) 30–60 cm), the bulk density, texture, pH, and total reserve cations (TRC) were determined (n = 29). The bulk density was determined using the cylinder method. The inner cylinder containing an undisturbed soil core was removed and trimmed to the end with a knife to yield a core whose volume could be easily calculated using its length and diameter. The

weight of this soil core was then determined after drying in an oven at 105 °C for approximately 18–24 h (Sandoval et al., 2012). The soil texture was measured using the hydrometer method proposed by Bouyoucos (1962). The samples containing organic C contents > 5% were pretreated with 10% H_2O_2. The soil pH was determined potentiometrically in 25 mL of KCl 1 N (soil: solution ratio: 1:2.5) with a glass electrode using an HI2550 meter (Hanna Instruments, US). The total reserve in base cations was measured (TRB, the sum of total Ca, Na, K, and Mg, in $cmol_c\ kg^{-1}$) by following the protocols published by Herbillon (1986).

2.4. Data treatment, principal component analysis (PCA), model generation, and predictive model validation of $\delta^{13}C$

From the total dataset (*n* = 332), six samples were identified as outliers using a leverage × studentised residual plot, obtained using the Pirouette software (Infometrix, Bothell, WA, USA) and eliminated from the set. An initial investigation of the structure of the data was performed with the Pirouette software by a PCA. NIR spectra of all samples were analysed together to visualise spontaneous relationships and clustering among all samples, natural clustering in the data, and outlier samples.

For model generation, the spectroscopy data were pretreated to eliminate nonlinearities produced by light scattering. For NIRS of soil, these include variability in the light scattering due to soil roughness, aggregates, structure, and particle size. The raw NIRS data were treated by smoothing (Savitzky–Golay filter, 11 points), multiplicative scatter correction (MSC), normalisation, and mean centering. MSCs are the most widely used preprocessing techniques for

NIRS data. Artefacts or imperfections (e.g., undesirable scatter effects) are removed from the data matrix prior to data modelling (Rinnan et al., 2009). In the total dataset (332 samples), six samples from the Choshuenco site were identified as outliers using a leverage × studentised residual plot (using Pirouette software, Infometrix, Bothell, WA, USA) and eliminated from the set. Prediction models were created using the pretreated data. The first models were generated by partial least-squares (PLS) regression, a standard method in the multi-variate analysis (Martens and Naes, 1989). Leave-one-out cross validation was performed on the PLS model as an internal validation, which approximates the results that are likely to be obtained by an external validation. This method removes one sample from the training set, performs PLS regression on the remaining samples, predicts the value for the left-out sample, and then analyses the error. This process is repeated until every sample has been left out once. In this manner, the root mean square error of cross validation (RMSECV) is computed.

Using the pretreated data, a second set of models was generated using a random forest (RF) approach. RF implements the Breiman's RF algorithm for classification and regression based on a forest of trees using random inputs (Cutler et al., 2012). The RF was generated through regression using 500 trees and 1,534 variables (i.e., 1/3 of the total number of used waves lengths) at each split.

The capability of the model to predict $\delta^{13}C$ of SOM for samples outside the training set was evaluated as follows: 1/3 of the data (111 samples) were selected randomly as the validation set, while the remaining 2/3 of the data were

used to train the models. This was tested 100 times on randomly selected training and validation sets to evaluate the prediction abilities of the generated models within a single sample set.

The model performance was assessed based on the root mean square error of the prediction (RMSEP) of the validation set and based on the correlation between the predicted and measured $\delta^{13}C$ values. All data pretreatments and model generations were performed using R (version 3.6.2).

To investigate the origin of the predictability of $\delta^{13}C$ by NIR spectra, we carried out Pearson correlation analyses between $\delta^{13}C$ (measured by IRMS and predicted by the best PLS model) and several physicochemical variables (% C, % N, % clay, TRB). We used the NIR spectra (1100–2800 nm) to generate PLS models to predict these physicochemical variables. We visually compared the regression coefficients of these models to those of the best $\delta^{13}C$-predicting PLS model to identify potential shared wavelength bands between the models, which might indicate the causal correlation underlying the predictability of $\delta^{13}C$. As the physicochemical variables % N, % clay, and TRB were only available for the 0–10 cm, 10–30 cm, and in some cores, 30–60 cm intervals of one composite sample per site (n = 29), whereas NIR spectra and IRMS data were only available at a finer depth resolution (n = 332). The spectra and $\delta^{13}C$ values were averaged accordingly before the pretreatment and model validations were carried out as described above.

Unless indicated otherwise, all data pretreatments and model generations were carried out using the statistical software R 3.6.2 and packages “prospectr”, “pls”, “Chemospec”, “BBmisc”, “clusterSim”, “plsRglm”, and “radiant.data”.

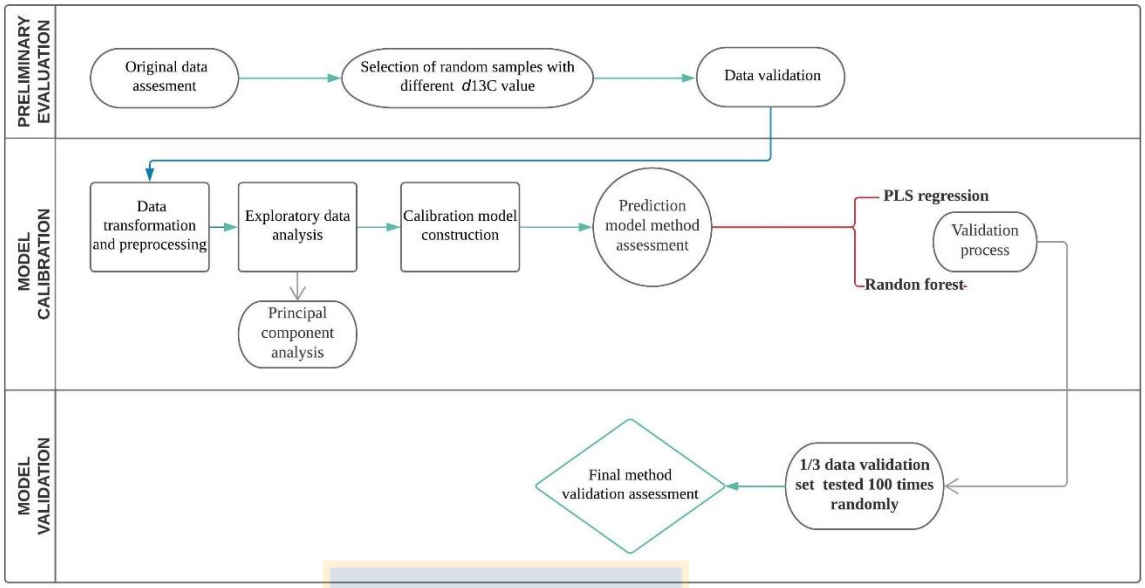

Figure 1. Flowchart of the model generation

3. RESULTS

3.1. Sites and soil-selected characteristics

The climatic and soil taxonomic variety of the soils included in this study is illustrated in Table 1. Table 2 shows the physicochemical variation that the soils in this study covered. Generally, the carbon and nitrogen contents decreased with the depth. Large differences between the locations were observed. The clay content also varied along the transect and it was in the range of 8 to 32%. Low bulk densities (< 1g cm^{-3}) were associated to Andisols and Inceptisols.

3.2.1. PCA as a clustering method

Figure 2 shows a score plot of the first two principal components of a single PCA. The panels in Fig. 2a, b are coloured based on different criteria (for example, moisture and temperature regimes) using some of the data in Table 1. However, this information did not force sample distribution because PCA is an unsupervised pattern recognition method. In SMRs, it is possible to observe clustering between the same moisture regimes. Xeric soils (blue) seemed to be separated from perudic soils by PC2 (variance: 7.1%) and partially separated from udic soils by both PC1 and PC2. Udic soils were also separated from perudic soils by the contribution of the two PCs. In STRs, it is also possible to observe separate clusters in thermic, mesic, and cryic soils, while isomesic samples appear evenly scattered in the space described by the first two PCs. The similarity between soils with isomesic and mesic regimes is attributed mainly to their comparable mean annual soil temperature ranges. Another clustering pattern showed that mesic soils (grey) seemed to be separated from thermic soils by PC2. Similarly, the thermic regime (orange) in Fig. 2b and xeric regime (blue) in Fig. 2a are separated by PC2.

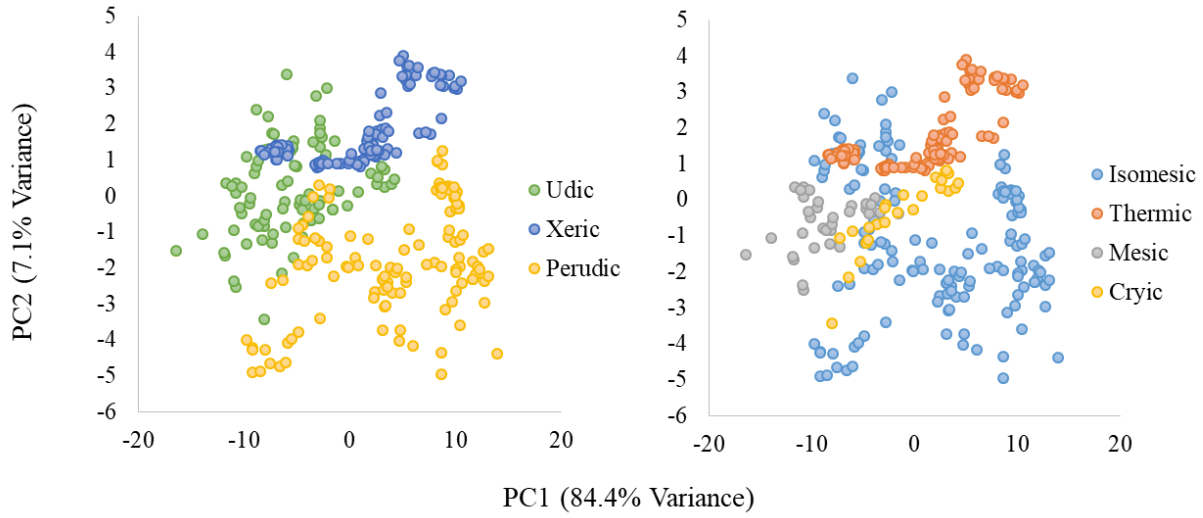

Figure 2. PCA plots based on the NIR spectra of all samples used in this study (*n* = 332). a) SMR and b) STR plots.

3.2.2. NIRS as a predictive method

The $\delta^{13}C$ values (−31 to −21.5‰), obtained by EA–IRMS, were used to train and validate the models. The average RMSECV and RMSEP of the PLS models for 100 randomly selected training (2/3 of the dataset) and validation (1/3 of the dataset) sets as functions of the number of latent variables (LVs) are shown in Fig. 3. Both RMSECV and RMSEP decreased with the increase in the number of LVs. The RMSEP of the model with five LVs (1.65 ± 0.15‰) was only marginally better than that of a model where the average value of the calibration set was used as a single predictor for the validation set (RMSEP = 1.70 ± 1.29‰). Therefore, only PLS models with six to ten LVs are analysed below. The average absolute difference between RMSECV and RMSEP for more than

six LVs was 0.11 ± 0.08‰. Thus, RMSECV is a good predictor of the RMSEP (Fig. 3).

In general, the RF model was better than the PLS models (Fig. 3 and Table 3). The average RMSEP for 100 randomly selected validation sets was 1.14 ± 0.15‰, considerably better than that obtained by the PLS models.

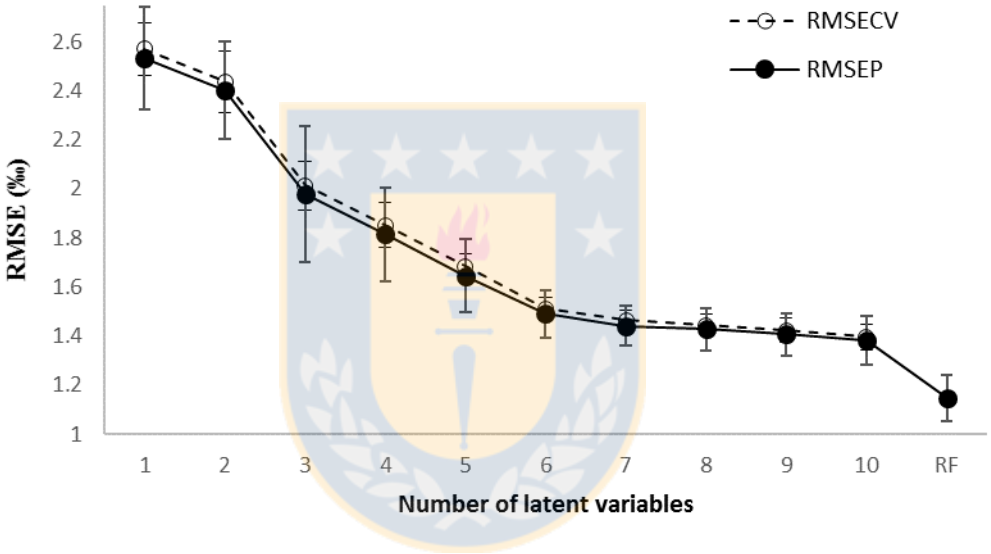

Figure 3. Averages and SDs of RMSECV and RMSEP for the PLS models as functions of the number of LVs and for the RF model determined using 100 randomly selected validation (111 samples) sets in the entire dataset (332 samples).

Notably, neither the $\delta^{13}C$ values measured by IRMS nor those predicted by the best PLS model correlated with the soil C and N contents, as shown in Fig. 4. However, the $\delta^{13}C$ values significantly correlated with the clay content ($r_{(PLS)}$ = 0.74, $r_{(IRMS)}$ = 0.76, $p < 0.05$, n = 24) and total reserve base ions ($r_{(PLS)}$ = 0.70, $r_{(IRMS)}$ = 0.62, $p < 0.05$, n = 24). The correlations between the $\delta^{13}C$ values

derived from the IRMS and prediction slightly differed, likely owing to the loss of variation upon their averaging to match the composite samples for which soil physicochemical data were available.

Table 3. Calibration and external validation performances of selected models. Average: a model using the average of $\delta^{13}C$ of the training set as a common value for all validation samples, #LV: number of LVs used to construct the PLS model, RMSEP (mean ± SD of 100 training iterations), R^2 (Pearson correlation for the predicted $\delta^{13}C$ as a function of the measured $\delta^{13}C$ of the validation sets), n.a.: not applicable.

	Validation	Random (1/3 of the dataset)		
Model type	# LV	Var	RMSEP	R^2
PLS	1	-87 ± 16 %	2.53 ± 0.21 ‰	0.1%
	2	-66 ± 18 %	2.40 ± 0.20 ‰	2.9%
	3	-6 ± 10 %	1.98 ± 0.28 ‰	23.5%
	4	11 ± 7 %	1.81 ± 0.19 ‰	28.6%
	5	26 ± 5 %	1.65 ± 0.15 ‰	40.4%
	6	40 ± 4 %	1.49 ± 0.10 ‰	48.3%
	7	44 ± 4 %	1.44 ± 0.08 ‰	49.8%
	8	48 ± 3 %	1.43 ± 0.09 ‰	49.2%
	9	55 ± 4 %	1.41 ± 0.09 ‰	51.6%
	10	59 ± 3 %	1.38 ± 0.10 ‰	54.1%
RF	n.a.	73%	1.15 ± 0.09 ‰	62.5%
Average	n.a.	n.a.	1.70 ± 1.29 ‰	n.a.

The performances of the PLS models for the prediction of % C, % N, % clay, and TRB were mediocre, owing to the limited sample sizes (% C: n = 332, 10 LVs, R^2 = 87.3, RMSEP = 1.92 ± 0.09 standard deviation (SD) %; % N: n = 29, 4 LVs, R^2 = 50.2, RMSEP = 3.61 ± 0.67 SD %; % clay: n = 29, 3 LVs, R^2 = 31.2, RMSEP = 8.86 ± 0.82 SD %; TRB: n = 29, 7 LVs, R^2 = 81.71, RMSEP = 4.88 ± 1.41.82 SD $cmol_c\ kg^{-1}$). However, this is not a major issue as these models were

generated only to visually compare their regression coefficients to those of the $\delta^{13}C$ PLS model.

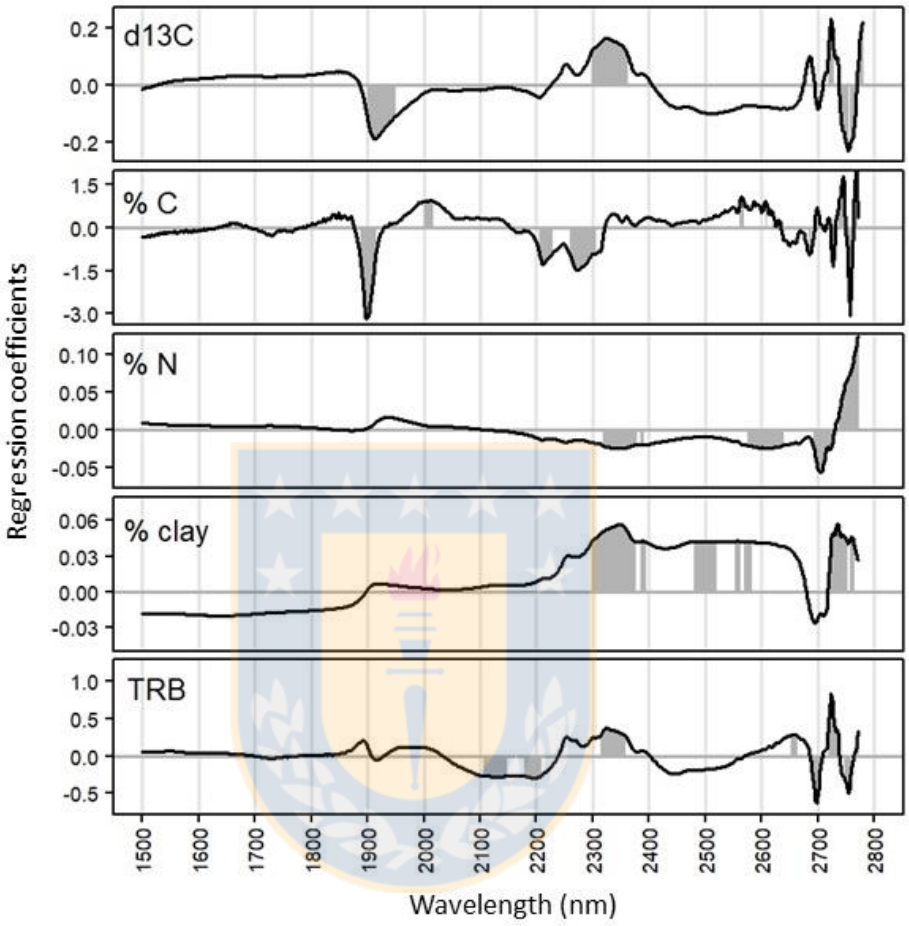

Figure 4. Regression coefficients of the NIR spectrum wavelengths used in the best PLS model to predict $\delta^{13}C$ as well as for the PLS models, which predict the soil C content (% C), soil N content (% N), clay content (% clay), and TRB. Only the wavelength range of 1500 to 2750 nm is shown, as the wavelengths below 1500 nm did not largely contribute to the models. A total of 10% of the wavelengths with the largest absolute regression coefficients in each model are highlighted in grey.

4. DISCUSSION

Climate can affect soil carbon storage by changing, through photosynthesis, plant biomass inputs; by affecting rates of enzymatic microbial decomposition; and by altering geochemical properties that can protect soil organic matter from decomposition (Davidson, 2015). The interactions of climatic and geochemical factors control soil organic carbon storage and turnover in grasslands (Doetterl et al. 2015); but soil organic C density (SOCD) and its driving factors are also depending of the ecosystems and soil depth examined (Wang et al. 2013; Guan et al. 2019). Wang et al (2013) found that soil organic carbon and $\delta^{13}C$ were correlated with soil characteristics across different ecosystems (e.g. forest; meadow, steppe; croplands) and concluded that SOCD is a key contributor to the variation of soil $\delta^{13}C$. The spatial representation of the sampling sites in their study and in ours to cover spatial variability of soil organic carbon and $\delta^{13}C$ across wide transects is challenging.

The stable isotope ratios of the life science elements carbon, hydrogen, oxygen, and nitrogen vary slightly, but significantly in major compartments of the earth (Ghosh and Brand, 2003). They provide a method to quantify the contributions of different components to the ecosystem exchange. ^{13}C natural abundance measurements have helped understand soil carbon dynamics and develop kinetically defined SOC pool sizes and turnover rates (Paul, 2016). Better understanding of soil carbon dynamics is essential to understand the roles of soil carbon in the carbon cycle and feedback mechanisms in climate changes. Thus, the measurement of soil carbon dynamics requires an accurate

assessment of isotopic variations, which can be distinguished by mass spectrometric measurements of soil samples (Ghosh and Brand, 2003). However, low-cost soil analysis alternatives are needed because the number of samples needed in such studies is large. Our study included different soil types and profiles under different environmental conditions to calibrate a predictive model and estimate $\delta^{13}C$ using NIRS, which covers a larger environmental gradient.

Exploratory analysis results (PCA) showed that the NIR spectra of the soils cluster is based on climatic regimes (Fig. 2) indicating that the climate shapes the soil physicochemistry, as reflected in the NIR spectra. Thus, the chemical information contained in the spectra is correlated with environmental variables. The PLS approach is a standard method in chemometrics (Wold et al. 2001), and it is a common regression method used to predict $\delta^{13}C$ (Martens and Naes, 1989). RFs have been successfully used for various applications in several disciplines. They provide a multi-purpose method that is applicable to both regression and classification problems, including multi-class classification (Cutler et al. 2012). NIRS calibration data for ^{13}C EA–IRMS (Table 3) show that it is possible to generate a suitable predictive model. Our primary concern was to select the correct method for the generation of a model to predict $\delta^{13}C$ in Chilean soils. We used RMSEP to assess the number of chosen components, so that the model has adequate information to provide reliable predictions. Conversely, if too many components are chosen, the model would have noise as well as information, which would lead to less reliable predictions to be included to maximise the prediction capacity of the model and avoid over-fitting.

The edaphoclimatic conditions in Chile are extremely variable. Thus, reliability is important for the development of a model for this type of transect. A model trained with soils having a large physicochemical variability is required. We evaluated the performances of the two methods for NIRS-based $\delta^{13}C$ prediction by their RMSEP values. RMSEP is a helpful measure of accuracy because it reflects the average differences between the measured and predicted values. Therefore, the model with more components was selected for PLS regression (Table 3, Fig. 3). As for both models (PLS and RF), the whole dataset was used and split into 2/3 (fit) and 1/3 (validation) sets randomly (repeated 100 times), and our approach provides a true assessment of the capability of the model to predict ^{13}C of samples within a sampling set. We evaluated the two methods for generation of models based on the validation set performances and qualities of the $\delta^{13}C$ values predicted using the NIRS data. The RMSEP values of the RF and PLS (with ten LVs) models were 1.15‰ and 1.38‰, respectively. Winowiecki et al. (2017) used similar models for soils in Africa under C3 and C4 plant species and obtained RMSEP = 1.95 and R^2 = 0.80 using PLS regression. For the RF approach, RMSEP was 1.77 and R^2 was 0.84. The R^2 values of the RF and PLS (with ten LVs) models were 62.5 and 54.1, respectively (Table 3). Our results are similar to those reported by Winowiecki et al. (2017) and Fuentes et al. (2012). In the three studies, the samples represent various conditions, such as vegetation classes (Winowiecki et al. 2017), crop residues and rotations (Fuentes et al. 2012), and edaphoclimatic conditions (ours). The results obtained in these studies favour the use of NIRS as a predictive method,

providing stable and rapid readings of ^{13}C in SOC. In this study, we further showed that the use of NIRS for $\delta^{13}C$ prediction is feasible at different soil depths along large transects with diverse soil types across Chile, which supports the studies on carbon dynamics in soils during climate changes.

To investigate the origin of the predictability of $\delta^{13}C$ by NIR spectra, we analysed the regression vectors of the $\delta^{13}C$-predicting PLS model and compared it to models predicting the soil C and N contents, clay content as a proxy for physical and chemical weathering, and total reserve base ions as a proxy for chemical weathering. The regression vectors of the models consist of the regression coefficients of all wavelengths in the NIR spectra, and thus reflect the importance of a given wavelength for the prediction of the various response variables (Fig. 4). The spectra start at 2778 nm in the MIR range, which is known to be related to signals from O-H vibration of acid groups, which can be related to degradation. The $\delta^{13}C$ model draws influential information around 2753 nm and 2723 nm. These peaks are also important for prediction of soil C content, TRB, and clay. The influential pattern between 2150 – 2400 nm is shared with the models predicting clay and TRB, while it does not fit the pattern of C and N prediction. This band of wavelengths is known to correspond with combinations of vibrations of C-H and C-C (Stenberg et al. 2010). A strong negative peak between 2000 - 1800 nm is partly shared with the model predicting soil C. This region is typically considered to correspond with the overtone of C=O and combinations with O-H stretching (O-H stretching is not informative, but the resulting adsorption can be combination with a C-C or C-H

or C-O stretches that are relevant) (Stenberg et al. 2010). We thus found indications that the prediction of $\delta^{13}C$ values draws its most influential information from the same NIR ranges as the prediction of soil C, clay content and total reserve base ions. This, together with the strong correlation of $\delta^{13}C$ values with clay content and TRB, suggests that $^{13}C/^{12}C$ ratio of SOC may be related to soil mineralogical properties, and that thus also the spectral prediction of $\delta^{13}C$ works in parts via this correlative relationship. Possible mechanisms could be that soil mineralogical properties affect carbon decomposition via physical or chemical protection (Davidson, 2015, Doetterl et al. 2015) which in turn is known to affect $\delta^{13}C$ values of SOM (Accoe et al. 2003).

According to Zornoza et al. (2008), high demands exist for rapid and predictive soil data acquisitions in environmental monitoring, soil quality assessment, and emerging methods of soil analysis. They correlated the soil fertility and physical and biological properties using NIRS. In this study, we obtained good predictions for the two selected models, and then, based on RMSEP and R^2, the RF model was chosen as the best model.

NIRS is considerably more affected by the physical structure variability caused by unrelated parameters, such as soil roughness, aggregates, structure, and particle size (size of aggregates, porosity, water) (Bellon-Maurel and Mc Bratney, 2011; Reyna et al. 2017), in comparison to Mid-Infrared (MIR) spectroscopy, which is another low-cost and easy-to-use alternative technique, NIR requires a simpler sample preparation than that of MIR. A strong further advantage of NIR is that is already widely established for quantification of a wide

range of soil properties (Reeves and McCarty, 2001; Blanco and Villarroya, 2002; Gómez, 2008).

NIR spectra were used to obtain a regression model. Abundant information is contained in the spectral data. However, only a few variables are necessary to obtain a good correlation with the predicted property (in this case, $\delta^{13}C$). For reliability of this technique, it is necessary to include a large number of samples from zones with wide ranges of values of soil properties (Zornoza et al. 2008). In this study, we covered various soils, which largely differed in different properties, and we used them to correlate the spectral data to ^{13}C. Thus, the calibrations are valid for numerous important environmental systems. According to Eiler (2013), “historical precedence suggests that no emerging analytical capability grows to its full potential unless it meets a serious need in the applied sciences”.

5. CONCLUSION

A prediction model for $\delta^{13}C$ based on NIRS data was developed using the PLS regression and RF approaches. Better results were obtained by the latter approach. The RMSEP parameters of both models indicated that NIRS can be used to predict $\delta^{13}C$ for various soil profiles. The model performances were high for the sample prediction using NIRS when the samples originated from the same sample set as the training set. The stable and rapid readings of ^{13}C of SOC obtained in this study support the use of NIRS as a predictive method in soil analysis and as a nondestructive waste-free method for the studies on carbon dynamics in soil. It was concluded that the predictability of $\delta^{13}C$ in soils

may be linked to its correlation with soil mineralogical properties, for which variables such as the clay content and total reserve base ions are proxies.

Acknowledgments

This study was supported by the government of Chile through the Regular Fondecyt Project N° 1161492. We acknowledge the Laboratory of Chemical Analysis of Soils and Plants of the University of Concepción for the support in the chemical characterisation of soils.

References

Accoe, F., Boeckx, P., Cleemput, O. V., Hofman, G. 2003. Relationship between soil organic C degradability and the evolution of the $\delta^{13}C$ signature in profiles under permanent grassland. Rapid communications in mass spectrometry, 17(23): 2591-2596.

Balesdent, J., Girardin,C., Mariotti, A. 1993. Site-related $\delta^{13}C$ of tree leaves and soil organic matter in a temperate forest. Ecology 74: 1713-1721.

Balesdent, J., Mariotti, A. 1996. Measurement of soil organic matter turnover using ^{13}C natural abundance. In Boutton, T.W., Yamasaki, S, Eds., Mass Spectrometry of Soils, New York: Marcel Dekker, 83-111.

Blanco, M. and Villarroya, Ignacio. 2002. NIR spectroscopy: a rapid-response analytical tool. Trends in Analytical Chemistry 21: 240-250.

Bouyoucos, G. J. 1962 Hydrometer method improved for making particle size analysis of soils. Agronomics Journal 54: 464-465.

Bricklemyer, R. S., Miller, P. R., Paustian, K., Keck, T., Nielsen, G. A., Antle, J. M. 2005. Soil organic carbon variability and sampling optimization in Montana dryland wheat fields. Journal of Soil Water Conservation 60: 42–51.

Carvalhais, N., Forkel, M., Khomik, M., Bellarby, J., Jung, M., Migliavacca, M., Reichstein, M. 2014. Global covariation of carbon turnover times with climate in terrestrial ecosystems. Nature, 514: 213-217.

Chabbi, A., Kögel-Knabner, I., Rumpel, C. 2009. Stabilised carbon in subsoil horizons is located in spatially distinct parts of the soil profile. Soil Biology & Biochemistry 41: 256–261.

Chen, Q., Shen, C., Sun, Y., Peng, S., Yi, W., Li, Z. A., Jiang, M. 2005. Spatial and temporal distribution of carbon isotopes in soil organic matter at the Dinghushan Biosphere Reserve, South China. Plant and Soil 273(1-2): 115-128.

Crowther, K. E., Todd-Brown, O., W. Rowe, C., Wieder, W. R., Carey, J. C.,. Machmuller, M. B., Snoek, B. L, Fang, S., Zhou, G., Allison, S. D., Blair, J. M., Bridgham, S. D., Burton, A. J., Carrillo, Y., Reich, P. B., Clark, J. S., Classen, A. T., Dijkstra, F. A., Elberling, B., Emmett, B. A., Estiarte, M., Frey, S. D., Guo, J., Harte, J., Jiang, L., Johnson, B. R., Kröel-Dulay, G., Larsen, K. S., Laudon, H., Lavallee, J. M., Luo, Y., Lupascu, M., Ma, L. N., Marhan, S., Michelsen, A., Mohan, J., Niu, S., Pendall, E., Peñuelas, J., Pfeifer-Meister, L., Poll, C., Reinsch, S.,. Reynolds, L. L, K. Schmidt, I., Sistla, S., Sokol, N. W., Templer, P. H., Treseder, K. K., Welker, J. M., Bradford, M. A.. 2016. Quantifying global soil carbon losses in response to warming Nature Letter Research 540: 104-108.

Cutler, A., Cutler, D.R. and Stevens, J.R. (2012) Random forests. In: Zhang, C. and Ma, Y.Q., Eds., Ensemble Machine Learning, Springer, Boston, MA.

Doetterl S, Berhe A, Arnold C, Bodé S, Fiener P, Finke P, Fuchslueger L, Griepentrog M, Harden W, Nadeu E, Schnecker J, Trumbore S, Van Oost K, Vogel C, Boeckx P 2018. Links among warming, carbon, and microbial dynamics mediated by soil mineral weathering. Nature Geoscience 11: 589–593.

Doetterl, S., Stevens, A., Six, J., Merckx, R.,Van Oost, K., Casanova Pinto, M., Casanova-Katny, A., Muñoz, C., Boudin, M., Zagal Venegas, E. Boeckx, P. 2015. Soil carbon storage is controlled by interactions between geochemistry and climate. Nature Geoscience 8: 780-783.

Davidson, E. A. 2015. Soil carbon in a beer can. Nature Geoscience 18: 748-749.

Eiler J.M. 2013. Isotopic Anatomies of Molecules and Minerals Annual Review of Earth and Planetary Sciences 41:411–41.

Finke, P., Opolot, E., Balesdent, J., Berhe, A. A., Boeckx, P., Cornu, S., Harden, J., Hatté, C., Williams, E., Doetterl, S., 2019. Can SOC modelling be improved by accounting for paedogenesis?. Geoderma 338: 513-524.

Fontaine, S., Barot, S., Barre, P., Bdioui, N., Mary, B., Rumpel, C., 2007. Stability of organic carbon in deep soil layers controlled by a fresh carbon supply. Nature 450: 277–281.

Fuentes, M., Hidalgo, C., González-Martín, I., Hernández-Hierro, J. M., Govaerts, B., Sayre, K. D., Etchevers, J. 2012. NIR spectroscopy: An alternative for soil analysis. Communications in Soil Science and Plant Analysis 43(1-2): 346-356.

Ghosh P, Brand W. A. 2003. Stable isotope ratio mass spectrometry in global climate change research International Journal of Mass Spectrometry 228: 1–33.

Glaser, B. 2005. Compound-specific stable isotope ($\delta^{13}C$) analysis in soil science. Journal of Plant Nutrition and Soil Science 168(5):–633-648.

Gomez, C., Rossel, R. A. V., and McBratney, A. B. (2008) Soil organic carbon prediction by hyperspectral remote sensing and field vis-NIR spectroscopy: An Australian case study. Geoderma, 146 (3-4): 403-411.

Guan, Jin-Hong., Deng, Lei., Zhang, Jian-Guo., He, Qiu-Yue,. Shi, Wei-Yu., Li, Guoqing., Du, Sheng. 2019. Soil organic carbon density and its driving factors in forest ecosystems across a northwestern province in China. Geoderma 352:1-12.

Herbillon, A. J. 1986. In Proc. 8th Int. Soil Classification Workshop (eds Beinroth, F. H., Camargo, M. N. & Eswaran, H.) 39–48 (EMBRAPA-SNLCS, 1986).

Kuzyakov, Y., Biriukova, O., Turyabahika, F., Stahr, K. 2001. Electrostatic method to separate roots from soil Journal of Plant Nutrition and Soil Science 164: 541-545.

Lal, R. 2006. Soil carbon sequestration in Latin America pp. 49-64. In: Lal, R. et al. (eds.) Carbon sequestration in soils of Latin America The Haworth Press, Binghamton, New York, USA

Martens, H. and Naes, T. 1989. Multivariate calibration Johnson Wiley & Sons, Chichester.

Mooney, S., Antle, J., Capalbo, S., Paustian, K., 2004. Influence of project scale and carbon variability on the costs of measuring soil carbon credits Environmental Management 33: S252–S263.

Paul E. A. 2016. The nature and dynamics of soil organic matter: Plant inputs, microbial transformations, and organic matter stabilisation. Soil Biology and Biochemistry 98: 109-126.

Petisco, C., García-Criado, B., Mediavilla, S., Vázquez De Aldana, B. R., Zabalgogeazcoa, I., García-Ciudad, A. 2006. Near-infrared reflectance spectroscopy is a fast and non-destructive tool to predict foliar organic constituents of several woody species. Analytical and Bioanalytical Chemistry 386 (6): 1823-1833.

Reeves, J.B. and McCarty, G.W. 2001. Quantitative Analysis of Agricultural Soils Using near Infrared Reflectance Spectroscopy and a Fibre-Optic Probe. Journal of Near Infra-red Spectroscopy 9: 25-34.

Reyna, L., Dubé, F., Barrera, J.A., Zagal, E., 2017. Potential model overfitting in predicting soil carbon content by visible and near-infrared spectroscopy. Applied Science 7: 708.

Rinnan, A., Van den Berg, F., Engelsen, B. 2009. Review of the most common pre-processing techniques for near-infrared spectra. Trends in Analytical Chemestry 28 (10): 1201–1222.

Rumpel, C., Kögel-Knabner, I., Bruhn, F., 2002. Vertical distribution, age, and chemical composition of organic carbon in the two forest soils of different paedogenesis. Organic Geochemistry 33: 1131–1142.

Sandoval, M., Dörner, J., Seguel, O., Cuevas, J., Rivera, D. 2012. Physical soil analysis methods, Department of Soils and Natural Resources Universidad de Concepción. Publication No. 5, 80p

Stenberg, B., Viscarra Rossel, R. A., Mouazen, A. M., Wetterlind, J. 2010. Visible and near-infrared spectroscopy in soil science. Advances in Agronomy 107: 163:215.

Trumbore, S. 2009. Radiocarbon and soil carbon dynamics. Annual Review of Earth and Planetary Sciences 37 (1): 47-66.

Viscarra Rossel, R. A., Walvoort, D., McBratney, A. B., Janik, L. J., Skjemstad, J. O. 2006. Visible, near-infrared, mid-infrared, or combined diffuse reflectance spectroscopy for simultaneous assessment of various soil properties. Geoderma 131(1-2): 59-75.

Viscarra Rossel, R.A., McBratney, A.B., 1998. Laboratory evaluation of a proximal sensing technique for simultaneous measurement of clay and water content. Geoderma 85 (1): 19– 39.

Shaoqiang Wang, Jiangwen Fan, Minghua Song, Guirui Yu, Lei Zhou, Jiyuan Liu, Huaping Zhong, Lupeng Gao, Zhongmin Hu, Weixing Wu, & Ting Song. 2013. Patterns of SOC and soil ^{13}C and their relations to climatic factors and soil characteristics on the Qinghai–Tibetan Plateau. Plant and Soil 363: 243-255.Winowiecki, L. A., Vågen, T., Boeckx, P., Dungait, J., 2017. Landscape-scale assessments of stable carbon isotopes in soil under

diverse vegetation classes in East Africa: application of near-infrared spectroscopy Plant and Soil 421(1-2): 259-272.

Wold, S., Sjöström, M., Eriksson, L., 2001. PLS-regression: a basic tool for chemometrics. Chemometrics and Intelligent Laboratory Systems 58:109–130.

Zornoza, R., Guerrero, C., Mataix-Solera, J., Scow, K.M., Arcenegui, V., Mataix-Beneyto, J. 2008. Near infra-red spectroscopy for the determination of various physical, chemical, and biochemical properties in Mediterranean soils. Soil Biology & Biochemistry 40: 1923-1930.

III. CAPITULO 3

PREDICTING SOIL ORGANIC CARBON MINERALIZATION RATES USING $\delta^{13}C$, ASSESSED BY NEAR INFRARED SPECTROSCOPY, IN DEPTH PROFILES UNDER PERMANENT GRASSLAND ALONG A LATITUDINAL TRANSECT IN CHILE.

Hidalgo Marcela[1,2], María de los Ángeles Sepulveda[2], Cristina Muñoz[2], Manuel Casanova[3], Daniel Wasner[4], Sebastian Doetterl[4], Samuel Bodé[5], Pascal Boeckx[5], Erick Zagal[2]*.

1 Agronomy Sciences Doctoral Program, Faculty of Agronomy, University of Concepción, Chile.
2 Department of Soil and Natural Resources, Faculty of Agronomy, University of Concepción, Chile
3 Department of Engineering and Soil, Faculty of Agronomics Science, University of Chile, Santiago, Chile.
4 ETH Zurich | ETH Zürich · Department of Environmental Systems Science
5 Isotope Bioscience Laboratory—ISOFYS, Ghent University, Belgium
* Correspondence Author: ezagal@udec.cl

Artículo publicado en Journal of Soil Science and Plant Nutrition (2022): 1-13.

https://doi.org/10.1007/s42729-022-00797-w

ABSTRACT

Purpose: Carbon (C) mineralization and turnover in soil relies on complex interactions among environmental variables that differ along latitudinal gradients. This study aims to quantify the relationship between the variation in $\delta^{13}C$ signature with soil depth ($\Delta\delta^{13}C$) and soil C turnover across a large geo-climatic gradient.

Methods: Thirteen grassland sites were sampled along a 4000 km latitudinal gradient in Chile. Maximising climatic and physicochemical soil's diversity to test the index with the widest range of application. We used near-infrared spectroscopy (NIRS) to estimate $\delta^{13}C$ of SOC at several soil depths. To assess soil C mineralization rates (CMR) and specific potential respiration (SPR) as proxies for C mineralization and turnover, using $\Delta\delta^{13}C$, soil incubations were performed.

Results: Highest ^{13}C isotope abundance was found at low latitude (-22.57 ‰, 35.5°S) and lowest at high latitude (-27.73 ‰, 53.2°S). Our results show ^{13}C's enrichment in parallel with decreasing C content with depth. The analysis of the relationship between $\Delta\delta^{13}C$ values versus CMR and SPR showed a significant positive relationship across all data points ($p<0.0001$, $R^2= 0.62$, $p<0.01$, $R^2= 0.29$, respectively). Partial correlation analysis of control variables indicates a relationship between $\Delta\delta^{13}C$ with CMR and SPR when controlling for climatic and soil physicochemical variables.

Conclusions: $\Delta\delta^{13}C$ calculated from NIRS´s may serve as a proxy to research the potential degradability of SOM and its interaction with soil geochemistry. Uncertainty and variability in the prediction power of our model reveals the importance of considering the latitudinal changeability in soil types as a control on properties controlling $\Delta\delta^{13}C$.

Keywords: C mineralization, NIRS, $\delta^{13}C$ signature, latitudinal gradient, specific potential respiration, soil profiles

1. INTRODUCTION

Soils represent the largest terrestrial carbon (C) reservoir (Jackson et al. 2017; Luo et al. 2017; Wang et al. 2018), but global distribution of soil organic carbon (SOC) is heterogeneous and depends upon soil type, soil microbial activity, land use, and climatic constraints. At the global scale, understanding of soil C decomposition processes, as well as the factors controlling them has increasingly become a matter of interest for land surface models predicting responses and developments of terrestrial C cycle, as well as remediation strategies for critical areas in the context of climate change (Singh et al. 2018). Thus, an easy-to-use and cost-effective techniques for estimating soil carbon degradability under different geoclimatic conditions and soil type are useful and needed. Moreover, most of the studies on soil organic matter (SOM) decomposition are on surface soils (Doetterl et al. 2015; Luo et al. 2017;

Ramírez et al. 2020; Singh et al. 2018) and less is known about C dynamics in subsoils (Doetterl et al. 2018; Dwivedi et al. 2017; Sheikh et al. 2020; Wynn et al. 2005).

Carbon decomposition mechanisms in soil involve complex interactions among environmental constrains like, climate, carbon inputs, soil properties and soil carbon fractions (Luo et al. 2016; 2017). As well as how the heterotrophic respiration reacts to changes in climate (Jones et al. 2005). Under certain geo-climatic conditions and vegetation, storage of SOC with minerals can be highly effective, becoming soil a C sink (Doetterl et al. 2015), since physical protection of soil C from microbial decomposition occurs when it is adsorbed onto aluminosilicate secondary mineral surfaces, which are formed by the weathering of rocks and soil minerals. Potential critical areas, which are zones with high SOC content and sensitive to climate change can become a source of greenhouse gas emissions (Lefèvre et al. 2017). In this sense, one of the most spacious land covers globally with significant SOC stocks are grasslands, which hold about 20% of SOC global stock within the first meters of soils (Lefèvre et al. 2017). Given the large variability of environmental conditions in which grasslands can occur, studies on latitudinal transects to understand these interactions at larger scales are useful to predict C dynamics. Recent studies on factors controlling C storage highlight the importance to understand interactions between geochemistry (all the aspects and processes of geology that involve a chemical change (Van der Watt & Van Rooyen, 1990) and climate for C dynamics in grasslands (Doetterl et al. 2015; Wang, 2017).

A relatively new method to assess C dynamics is quantifying variations in the $^{13}C/^{12}C$ ratio of SOC with soil depth and across soil regions (Accoe et al. 2003; Ågren et al. 1996 Jones et al. 2009; Poago & Feng, 2004; Wang et al. 2017; 2018). Stable carbon isotopes composition of natural abundance has shown to be useful to examine, among others, ecological, biological, and geochemical processes related to ecosystems; providing information at temporal and spatial scale on C dynamics (Poage, 2004; Tcherkz et al. 2011). About 98.89% of all C in nature is ^{12}C, and 1.11% is ^{13}C, and the ratio of the stable C isotopes in natural materials differs scarcely around these average values. As a result of isotopic fractionation during physical and biochemical processes, like photosynthesis and the consequential reactions of anabolism and catabolism of organic carbon (OC), differences in isotope ratios provide information as a tracer in dynamic biological systems; that is applicable from a single biological process of living structures to terrestrial ecosystem processes (Boutton, 1991).

Isotopic methods are appropriate for tracing deep carbon dynamics, since absolute changes in carbon stocks and carbon fluxes in the deep soil horizons cannot be quantified by direct measurement. Usually, temporal variations in stocks are smaller than measurement accuracy. This is due to the very low carbon concentrations (e.g. less than 5 g kg^{-1} at depths of 80 cm), spatial heterogeneity and slow changes in time (Balesdent et al. 2018). Stable-isotope-based observation, are meaningful in estimating the proportions of active and stable carbon in soil (Balesdent and Mariotti, 1996) and the quantification of the recent incorporation of atmosphere-derived carbon atoms into whole-soil profiles

(Balesdent et al. 2018). Moreover, evidence on incoming fluxes resulting from root mortality and exudation/secretion by living roots is not accessible without tracers. Also, in situ quantification of soil respiration where the CO_2 efflux is the result of heterotrophic respiration and root autotrophic respiration would not be possible without the use isotope techniques (Boutton, 1991).

Normally, the determination for soil $\delta^{13}C$ for soil $\delta^{13}C$ is by elemental analysis - isotope ratio mass spectrometry, EA-IRMS, reported as the variation in the ratio $^{13}C/^{12}C$ relative to the Vienna PDB standard (Accoe et al. 2003; Boutton, 1991). Often differences of 0.1 $^{0}/_{00}$ are significant for palaeoclimatologists and geochemists (Boutton, 1991). Furthermore, even a small discrimination against ^{13}C, for example during respiration, could cause a substantial ^{13}C enrichment in time in the remaining substrate, once most of the original C of a litter cohort has been mineralised (Högberg et al. 2005). The ^{13}C abundance of SOM is mainly determined by the isotopic abundance of the plant litter source and its photosynthetic pathways. C3 plants present $\delta^{13}C$ signatures ranging from approximately -32 to -22 $^{0}/_{00}$, while C4 and obligate CAM (Crassulacean acid metabolism) plants present $\delta^{13}C$ values ranging from approximately -17 to -9 ‰ (Boutton, 1996; Tcherkez et al. 2011). Moreover, it has been widely described that $\delta^{13}C$ of SOM increases and C content concentration decreases with soil depth (Accoe et al. 2003; Brunn et al. 2015; Poage and Feng, 2004, 2002). Isotope accumulation of the heavier isotope (^{13}C) in the soil profile has been related to processes such as:

Isotopic fractionation during the microbial C mineralization. It results if microorganisms preferentially respire CO_2 that is ^{13}C-depleted relative to the substrate, and consequently in a ^{13}C enrichment of the remaining C (Accoe et al. 2003; Feng, 2002).

The Suess effect, corresponding to a gradual decrease of atmospheric $\delta^{13}C$ because of the increase of ^{13}C-depleted C through the burning of fossil fuel and deforestation since industrial revolution (Lichtfouse et al. 2003; Piotrowska et al. 2020; Wynn et al. 2004).

Aggregate's physical and chemical protection of polysaccharide material from the inputs of organic matter from leaves and roots that shows a wide range of isotopic values (from ^{13}C-depleted lignin to ^{13}C-enriched polysaccharides). The ^{13}C in aggregates is enriched with decreasing aggregate size (Brugnoli and Farquhar, 2000; Di & Huang, 2021; Tcherkez et al. 2011). On the other hand, the residual increase in $\delta^{13}C$ of the organic matter below a soil depth of 20 cm can result from the increased contribution of ^{13}C-enriched microbially derived C with depth (Boström et al. 2007). If ^{13}C-enriched polysaccharides do not preserve in soil, these labile compounds are converted to microbial compounds, which have slower turnover rates than plant components (Gleixner et al. 2002). It is known that microorganisms are ^{13}C-enriched by 2 – 4 ‰ compared to plant material (e.g., Wallander et al. 2004).

With growing data availability of $\delta^{13}C$ of SOM, this data is becoming more widely used to assess C dynamics. As such, crucial information could be obtainable from understanding enrichment of $\delta^{13}C$ in soil and help to predict processes

(e.g. C decomposition and identify critical areas to focus C stabilization strategies) that are relevant in the context of predictions and mitigation of the effect of further climate change (Bird et al. 1997; Powers et al. 2002; Ramírez et al. 2020).

In a pioneering study, Accoe et al. (2003) have proposed to use the change of $\delta^{13}C$ value with depth ($\Delta\delta^{13}C$) to establish relationships with mineralization rate and decomposition rate constant (k) as an indicator of SOC stability. However, since the study was limited in space and restricted to just a few soil types, it is unclear how the investigated relationship enfolds across chemically and physically different soil types, soil depth and varying geo-climatic conditions. Thus, more knowledge is required to better understand the potential C dynamics at the global scale, for example by studying latitudinal transects across a range of soil types and environmental settings. However, this demands a high number of soil samples to be analysed which can be time-consuming and expensive using conventional methods for soil $\delta^{13}C$ determination by (i.e., elemental analysis - isotope ratio mass spectrometry, EA-IRMS). The use of infrared diffuse reflectance spectroscopy in the near-infrared spectral range (NIRS) (Fuentes et al. 2012; Sepúlveda et al. 2021; Winowiecki et al. 2017) could provide a cost-efficient and fast alternative to traditional methods for assessing soil $\delta^{13}C$. In this regard, this study aims to test if $\Delta\delta^{13}C$ values estimated by NIRS in grassland soils can be used for assessing C mineralization rates (CMR) and the specific potential respiration (SPR) per unit C in soil sampled along a large latitudinal gradient across several soil types and geo-climatic regions at

varying depth. Doing so, we test if NIRS derived $\delta^{13}C$ can be used as an approach to predict the degradability of SOC and unveil the influence of climatic and geochemical factors on the capacity of $\delta^{13}C$ signature to predict soil C turnover.

2. MATERIALS AND METHODS

2.1 Study sites and soil sampling

Thirteen sites under natural grassland and/or shrubland were selected along a latitudinal transect across Chile, ranging from 32°S to 53°S. Criteria that were considered for site selection were chosen to cover a wide range of climatic and soil development stages to which SOC stocks respond in terms of size and lability. Thus, sites were chosen to maximise the climatic and physicochemical diversities of the soils to test the applicability of a $\delta^{13}C$-based approach to predict the degradability of SOC, with the widest range of application. Climatic zones covered by this study are mediterranean semiarid (MSA), temperate semi-oceanic (TSO), temperate oceanic (TO), sub-polar semi-oceanic (SPSO) and sub-polar dry (SPD) as described by Doetterl et al. (2015). Soil orders covered are Alfisols, Mollisols, Inceptisols, Andisols, Ultisols and Entisols (Table 1) developed from a variety of parent materials (e.g., volcanic ash, alluvial, fluvioglacial material, marine sediments), under different environmental conditions. Thus, selected soils varied both in soil moisture regimen (SMR) (aridic, xeric, udic and perudic) and soil temperature regimes (STR) (thermic,

mesic, isomesic and cryic) with diverse values of mean annual precipitation (MAP) and mean annual temperature (MAT) along the latitudinal gradient (Table 1); and covering a broad pHKCl range (3.9 - 5.8, Table 2). Field sampling campaigns for all sites were conducted during the summer season, close to the peak of the growing season in 2017 and 2018. At each site, 4 replicate plots of 50 x 50 m were established and six soil cores per plot distributed randomly across the plot were taken. PVC tubes (height: 35 cm; diameter: 90 mm) were used to extract undisturbed, depth explicit soil cores. Depending on the coarse rock content of the profiles, soil samples were either taken down to 30 cm (4 sites) or 60 cm depths (9 sites), completing a total of 52 soil cores samples. The tubes were transported (refrigerated) back to the laboratory and kept frozen (-18°C) until further processing.

2.2 Soil geochemical and physical analysis

To gather data for later calibration of NIRS spectra, geochemical and physical soil properties were assessed using traditional soil laboratory methods at 0-10; 10-30; and 30-60 cm depth. Here we report mainly those soil physical and chemical properties used in this study. Briefly, before analyses, samples were air-dried and sieved through a 2 mm sieve. Bulk density was determined using the Kopecky cylinder method (Blake & Hartge, 1986). Soil pH was determined potentiometrically in 1 M KCl (soil: solution = 1:2.5) with a glass electrode (HI2550 meter, Hanna Instruments, US), plus Al^{+3} exchange extractable with KCl 1mol L^{-1} and analysed by atomic emission and absorption spectrophotometry (SOLAAR 969). Selective extraction methods were used,

e.g., extraction with ammonium oxalate, where Fe_2O_3 and Al_2O_3 were determined. For the volcanic soils (Andisols), an extraction with sodium pyrophosphate was carried out, obtaining Fe_2O_3 and Al_2O_3, where the corresponding elements were determined by atomic absorption spectrometry (SOLAAR 969). Soil clay was measured using the hydrometer method for soil texture, after samples were pre-treated with 10 % H_2O_2 (Bouyoucos, 1962). Prior to C analyses, fine roots were removed using electrostatic energy, as described by Kuzyakov et al. (2001). The total organic carbon content (% C) and total nitrogen content (% N) was measured by dry combustion using an elemental analysis system (Truspec CN, LECO. USA). Inorganic C was not present in all soils (e.g., range of pH used for soil sampling and tested with HCl).

2.3 Soil organic C and NIRS predictions of $\delta^{13}C$ values

In a first study we tested NIRS to assess stable isotopes of C in soil (see, Sepúlveda et al. 2021) for fast screening of multiple samples (e.g., wide transect and at different depths). In this study, for similar soils, we tested the good relationship between the soil ^{13}C change with depth ($\Delta\delta^{13}C$) and C turnover observed by Accoe et al. (2003) for only 3 grasslands. As mentioned earlier, NIRS predictions of $\delta^{13}C$ data at 0-5; 5-10; 10-20; 20-30; 30-40 and 40-60 cm depth were obtained using the method developed in Sepúlveda et al. (2021). Briefly, as preparation for conducting NIRS measurements, three replicates of the six soil cores per plot were cut into slices of 2, 5 and 10 cm and air dried. The topsoil section (0 – 10 cm) was cut into five slices of 2 cm, the section from 10 to 30 cm into four slices of 5 cm, and the subsoil section from 30 to 60 cm

was cut into three slices of 10 cm. This resulted in 12 subsamples for the 60 cm cores, and 9 subsamples for the 30 cm cores. Soil organic carbon content and $\delta^{13}C$ of these subsamples was assessed using NIRS (800–2857 nm) by diffuse reflectance spectroscopy at 4 cm^{-1} resolution using a Fourier-transform NIR system (Bruker Matrix-I; Bruker Optics, Rheinstetten, Germany) in triplicate for each sample. From the total dataset (n = 332), an initial investigation of the structure of the data was performed with the Pirouette software (Infometrix, Bothell, WA, USA) by a principal component analysis (by a PCA.). NIR spectra of all samples were analysed together to visualise spontaneous relationships and clustering among all samples, natural clustering in the data, and outlier samples. For model generation, the spectroscopy data were pretreated to eliminate nonlinearities produced by light scattering. The raw NIRS data were treated by smoothing (Savitzky–Golay filter, 11 points), multiplicative scatter correction (MSC), normalisation, and mean centring. Artefacts or imperfections (e.g., undesirable scatter effects) are removed from the data matrix prior to data modelling. Prediction models were created using the pretreated data. The first models were generated by partial least-squares (PLS) regression. Leave-one-out cross validation was performed on the PLS model as an internal validation, which approximates the results that are likely to be obtained by an external validation. This method removes one sample from the training set, performs PLS regression on the remaining samples, predicts the value for the left-out sample, and then analyses the error. This process is repeated until every sample has been left out once. In this manner, the root mean square error of cross validation (RMSECV) is computed. Using the pretreated data, a second set of models was

generated using a random forest (RF) approach. RF implements the Breiman's RF algorithm for classification and regression based on a forest of trees using random inputs. The RF was generated through regression using 500 trees and 1.534 variables (i.e. 1/3 of the total number of used wave's lengths) at each split. The model performances were acceptable. The values of the root mean square error of prediction for the validation runs for $\delta^{13}C$ obtained using the PLS and RF models were 1.38 ‰, and 1.15 ‰, respectively. Model performance indicated that the NIRS can be used to predict $\delta^{13}C$ for the selected study area (see, Sepúlveda et al. 2021). PLS model has been used in soil studies before (Fuentes et al. 2012; Winowiecki et al. 2017).

2.4 C mineralization rates and specific potential respiration, and their relationship with the rate of change of $\delta^{13}C$ with increasing depth ($\Delta\delta^{13}C$ value)

To measure CMR and SPR, a 30 g composite soil sample were incubated for 60 days at 20°C in triplicate for the following depth intervals: 0-5 cm, 5-10 cm, 10-20 cm, 20-30 cm, 30-40 cm, and 40-60 cm depth. The composite soil sample was prepared from the same material and cores as used for calibrating the NIRS data. About 12 subsamples for the 60 cm cores, and 9 subsamples for the 30 cm cores. The composite sample for each interval was created as follows: the 0-5 cm, was made using 12 g from subsamples 1, 2; and 6 g from subsample 3; for interval: 5-10 cm using 12 g from subsamples 4, 5; the interval 10-20 cm was prepared with 15 g of subsamples 6 and 7; the same for interval: 20-30 cm, 15 g from subsample 8 and 9; the interval 30-40 cm was composed by 30 g from

Table 1. Description of the latitude, soil series, georeferenced (UTM), soil order; MAP, MAT, SMR, STR and climatic zones of the study sites.

Latitude	Soil series		zone 19 South		MAP	MAT	Soil climatic regimen		Soil taxonomy	Climatic zone
			E-UTM m	N-UTM m	mm/year	°C	STR	SMR		
31,9°S	Los Vilos		263342	6477586	208	16.4	isothermic	Aridic	Torric Psamment	Mediterranean semiarid (MSA)
32,8°S	Calle larga		357651	6361423	349	14.6	thermic	Xeric	Typic Argixeroll	
34,3°S	Pimpinela		340864	6200578	568	14.1	thermic	Xeric	Mollic Haploxeralf	
35,8°S	Matanza		234301	6237593	474	16.9	isothermic	Ustic	Oxic Haplustoll	
35,5°S	Bramadero		290355	6056474	869	13.9	thermic	Xeric	Humic Haploxerand	Temperate semi-oceanic (TSO)
36,6°S	Santa Bárbara		258294	5961851	1321	12	thermic	Xeric	Typic Haploxerand	
37,3°S	Carampangue		653701	5875605	1431	13.4	isomesic	Udic	Fluvaquentic Dystrudept	
42,1°S	Pachabrám		596724	5302714	2039	10.9	isomesic	Perudic	Histic Duraquand	Temperate oceanic (TO)
43,1°S	Aitiú		612611	5302714	2232	10.8	isomesic	Perudic	Hydric Fulvudand	
44,7°S	Puerto Cisne		688801	5041291	2501	9.7	isomesic	Perudic	Acrudoxic Fulvudand	Sub-polar semi-oceanic (SPSO)
46,6°S	B. Exploradores		643673	4849209	1134	6.2	mesic	Udic	Oxyaquic Hapludand	
53,2°S	Agua Fresca		368000	4080000	620	8.1	cryic	Udic	Inceptisol	Sub-polar dry (SPD)
53,3°S	Santa Olga		409570	4091863	483	6.3	isomesic	Perudic	Inceptisol	

Table 2. Summary of descriptive statistics (n, mean, standard deviation, minimum and maximum) of the geochemical characterization of the soil profiles across the latitudinal transect for selected depth intervals of (0-10; 10-30 and 30-60 cm).

Depth cm	Summary	C %	N %	Bulk density g cm^{-3}	Clay %	pH_{KCl} -	Al_2O_3 %	Fe_2O_3 %
0 - 10	n	13	13	13	13	13	13	13
	Mean	7.88	0.54	1.01	20.22	4.67	36,80	13,99
	S.D.	6.16	0.4	0.37	9.74	0.53	44,12	11,60
	Minimum	0.74	0.07	0.5	5.9	3.9	0,74	1,68
	Maximum	19.4	1.49	1.4	36	5.5	123,34	41,08
oct-30	n	13	13	13	13	13	13	13
	Mean	4.73	0.2	1.15	22.78	4.71	68,88	19,80
	S.D.	4.57	0.13	0.41	10.14	0.51	86,85	23,92
	Minimum	0.29	0.06	0.6	6.6	3.9	1,56	0,11
	Maximum	13.7	0.46	1.8	37.8	5.5	289,81	71,01
30 - 60	n	9	9	9	9	9	9	9
	Mean	4.01	0.18	0.84	20.76	4.84	136,44	36,27
	S.D.	3.82	0.13	0.35	9.45	0.54	132,35	35,17
	Minimum	0.32	0.01	0.4	6.6	3.9	3,00	1,89
	Maximum	12.7	0.41	1.6	35.5	5.8	377,48	88,80

subsample 10 and for the interval: 40-60 cm, 15 g of subsamples 11 and 12 were used. All in triplicate. The composite samples were first conditioned to 60 % water-filled pore space (WFPS, kept constant throughout the incubation) and pre-incubated for 10-days. During the actual incubation, soil respiration was measured periodically (1, 3, 7, 10, 15, 30, 45 and 60 days) using a CO_2 gas analyser (Li-820, Li-COR Bioscience, Lincoln, NE, USA). The Falcon tubes (50 ml) used for incubation were regularly aerated. We determined CMR (mg C kg^{-1} soil day^{-1}) as the slope of a linear regression fitted through the evolution of cumulative CO_2-C production between days 1 and 60. SPR was calculated as

the ratio of respiration and soil C content. Meanwhile, the average change of the $\delta^{13}C$ value per depth increment in each 10 cm depth interval ($\Delta\delta^{13}C$ value, expressed in ‰ cm^{-1}), was calculated as the slope of a linear regression of the evolution of the $\delta^{13}C$ values with depth.

2.5 Statistical analyses and correlations to geo-climatic controls

To assess the occurrence of NIRS $\delta^{13}C$ soil profile signature, CMR and SPR along the latitudinal gradient, a variance analysis (ANOVA) was performed with soil series and climatic zones as classification variables (n=70). Before the ANOVA analysis a Normal Score transformation data was carried out to ensure a normal distribution of the variables (Goovaerts, 2001; Liu et al. 2010), along with a Duncan post hoc test with a significance level of $p<0.05$. Then, to evaluate the capacity of $\Delta\delta^{13}C$ signature to predict CMR and SPR with increasing soil depth across the latitudinal transect a linear regression (n=52) was performed. Since $\Delta\delta^{13}C$ signature serve as a direct indicator of the degradability of the SOM in the soil profile. As it is inversely related to the stability of the SOM (Accoe et al. 2003). Following that, to estimate the effect of climatic and geochemical factors on influencing $\Delta\delta^{13}C$ as a predictor of CMR and SPR partial correlations were performed using the statistical software R (version 3.6.2), and packages “pco” and “plsRglm”. MAP (Table 1), SOC content, clay content, pHKCl, Fe and Al content (Table 2) were used as controls on the relationship of $\delta^{13}C$ and CMR, and SPR, and were applied for all soil depth together (n=26), at 0-10, 10-30 and 30-60 cm soil depth and compared to zero-order correlation between the latter variables without including controls.

3. RESULTS

3.1 $\delta^{13}C$ signature and SOC content along the geo-climatic gradient

From aridic to perudic/udic soil moisture regimes (Table 1), $\delta^{13}C$ value decreases in magnitude (Fig. 1) and shows a wider range of possible values with increasing depth (data not shown). Throughout the studied gradient, soils from MSA climate exhibited the highest ^{13}C isotope abundance (soil serie Matanza -22.257 ‰, 35.5°S).

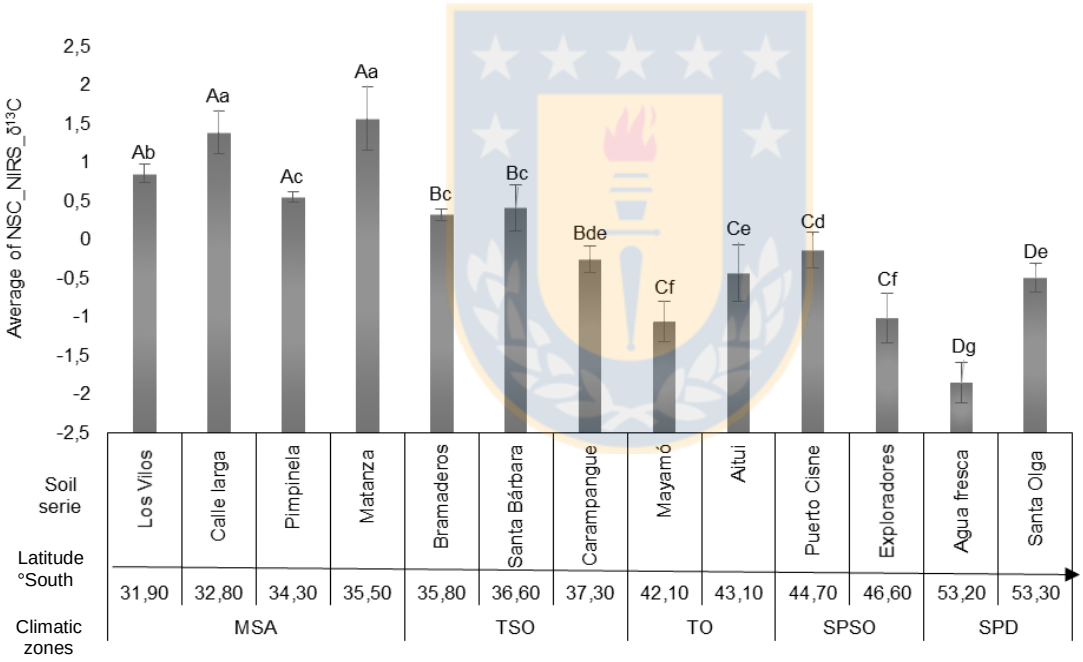

Fig. 1 Latitudinal gradient in the $\delta^{13}C$ value average (S.D. bars) of the soil samples analysed at different soil depth (from 0 to 60 cm). (Latitude reported as degree south and $\delta^{13}C$ as per mil deviations from the international PDB standard). Locations (soil series) and climate zones as explained in Table 1.

Lowest ^{13}C isotope abundance was observed for the SPD climate zone (soil serie Agua Fresca -27.73 ‰, 53.2°S). Average $\delta^{13}C$ value of the soil samples analysed at different soil depth (from 0 to 60 cm) for climatic zones analysis (n=70) and soil series analysis (n=70) are shown in Figure 1 and Table 3.

Table 3. Average values of C mineralization rate (CMR) (mg CO_2-C kg $soil^{-1}$ d^{-1}), Specific potential respiration (SPR) (mg CO_2-C g SOC^{-1} d^{-1}), NIRS predicted $\delta^{13}C$ values and their Normal Score (NSC) transformed data in the latitudinal gradient (degrees S) and climatic zones.

Climate	Latitude	soil serie	CMR	NSC_CMR	SPR	NSC_SPR	NIRS$\delta^{13}C$	NSC_NIRS$\delta^{13}C$
	°S		mg CO_2-C kg $soil^{-1}$ d^{-1}		mg CO_2-C g SOC^{-1} day^{-1}		($^0/_{00}$)	
MSA	31.9	Los Vilos	0.332	-1.037	0.060	0.902	-24.193	0.857
	32.8	Calle larga	1.026	0.183	0.030	0.228	-22.840	1.393
	34.3	Pimpinela	0.436	-0.348	0.025	0.030	-24.808	0.550
	35.5	Matanza	0.303	-0.680	0.005	-0.085	-22.578	1.570
TSO	35.8	Bramaderos	0.468	-0.827	0.025	-1.203	-25.082	0.323
	36.6	Santa Bárbara	0.573	-0.603	0.012	-0.670	-24.907	0.415
	37.3	Carampangue	1.049	-0.005	0.058	0.740	-26.062	-0.252
TO	42.1	Mayamó	1.728	0.527	0.017	-0.440	-26.953	-1.055
	43.1	Aituí	2.968	0.420	0.018	-0.627	-26.183	-0.435
SPO	44.7	Puerto Cisne	2.732	0.708	0.019	-0.547	-25.878	-0.135
	46.6	Exploradores	2.710	0.212	0.064	0.808	-26.850	-1.018
SPD	53.2	Agua fresca	5.527	1.015	0.116	1.553	-27.730	-1.855
	53.3	Santa Olga	3.619	1.078	0.028	0.108	-26.283	-0.493

For both variables, results were significant (R^2=0.94, p<0.0001; R^2=0.75, p<0.0001; climate and soil series respectively). Across all sites, and despite of the variability along the gradient, soil $\delta^{13}C$ showed a trend to increase with soil depth (Fig. 1). NIRS predicted $\delta^{13}C$ values with mean soil $\delta^{13}C$ values increased from -25.63 ‰ (±1.48 ‰ S.D.) to -25.11 ‰ (±1.42 ‰ S.D.) from top to subsoil (Table 4, Fig. 2). Deviations from the described trends (enrichment of $\delta^{13}C$ with depth, depletion of SOC with depth) were observed for soils with volcanic parent

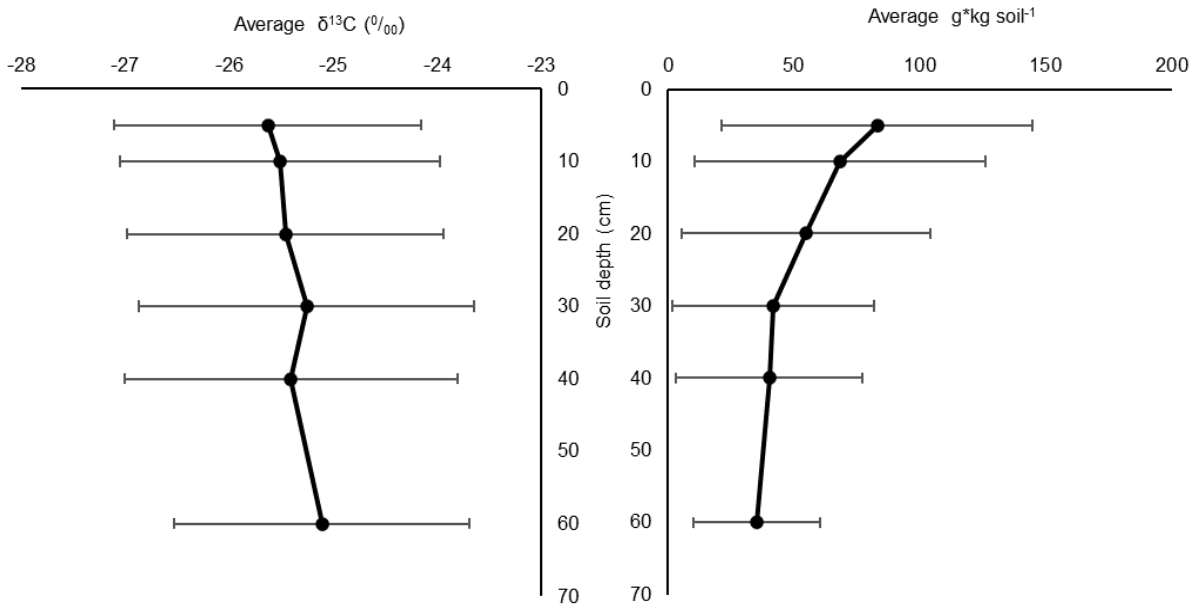

Fig. 2 Average C content and $\delta^{13}C$ abundance in function of depth of the latitudinal transect. including standard deviation bars. Depth increments; 0-5 cm (n=13); 5-10 cm (n=13); 10-20 cm (n=13); 20-30 cm (n=13); 30-40 cm (n=9); 40-60 cm (n=9).

materials and polygenetic soil profiles that could correspond to a different depositional stage of volcanic ash sediments (Dahlgren et al. 2004). Soils series Bramaderos, Santa Bárbara, Mayamó and Aituí, all of them Andisols, from temperate semi-oceanic and temperate oceanic climatic zone, that fall under these criteria exhibiting a higher standard deviation of the $\delta^{13}C$ average value (Fig. 1). Meanwhile, soil C content in topsoil (0-10 cm) assessed for all 13 soils ranged from 0.74 to 19.4 % with an average of 7.88 % (± 6.16 % S.D.). For 10-30 cm soil depth, values ranged from 0.29 to 13.7 % with an average of 4.73 % (±4.57 % S.D.); nine soils for which subsoil could be sampled (Entisol, Mollisol, Inceptisol and Andisol) (30-60 cm depth) ranged from 0.32 to 12.7 % with an average at 4.01 % (±3.82 % S.D.) (Table 2). Always, total C content decreased with depth as shown in Fig. 1.

Table 4. Summary of descriptive statistics for soil profiles across the geolatitudinal transect (n, mean, standard deviation, minimum and maximum) of C content, C mineralization rate (CMR), Specific potential respiration (SPR) and predicted $\Delta\delta^{13}C$ at depths of 0-5, 5-10, 10-20, 20-30, 30-40 and 40-60 cm.

Depth cm	Summary	C content g kg soil^{-1}	CMR mgCO$_2$-C kg soil^{-1} day^{-1}	SPR mgCO$_2$-C g SOC^{-1} day^{-1}	$\delta^{13}C$ ‰	Predicted $\Delta\delta^{13}C$ ‰ cm^{-1}
0-5	n	13	13	13	13	13
	Mean	83.07	4.88	0.06	-25.63	0.06
	S.D.	61.63	5.25	0.06	1.48	0.07
	Minimum	9.12	0.46	0.01	-27.91	-0.06
	Maximum	195.70	15.82	0.22	-22.97	0.20
5-10	n	13	13	13	13	13
	Mean	68.29	1.88	0.04	-25.51	0.05
	S.D.	57.88	1.40	0.03	1,54	0.05
	Minimum	7.40	0.29	0.01	-27.82	-0.03
	Maximum	173.30	4.14	0.10	-22.83	0.14
10-20	n	13	13	13	13	13
	Mean	54.82	1.27	0.03	-25.46	0.04
	S.D.	49.20	1.25	0.03	1.52	0.03
	Minimum	4.80	0.21	0.01	-27.64	-0.01
	Maximum	150.90	4.80	0.09	-22.76	0.09
20-30	n	13	13	13	13	13
	Mean	41.76	0.66	0.03	-25.26	0.04
	S.D.	40.03	0.55	0.02	1.61	0.03
	Minimum	2.90	0.13	0.01	-27.55	-4.0E-03
	Maximum	106.03	1.96	0.07	-22.23	0.09
30-40	n	9	9	9	9	9
	Mean	40.18	0.45	0.02	-25.41	0.02
	S.D.	37.09	0.47	0.02	1.60	0.01
	Minimum	2.54	0.15	4.0E-03	-27.42	2.0E-03
	Maximum	95.80	1.35	0.06	-22.20	0.04
40-60	n	9	9	9	9	9
	Mean	35.33	0.29	0.02	-25.11	0.01
	S.D.	25.21	0.18	0.02	1.42	0.03
	Minimum	3.20	0.11	2.0E-03	-26.39	-0.04
	Maximum	75.60	0.62	0.05	-22.12	0.04

3.2 C mineralization rates, specific potential respiration gradient analysis, and their relationship to $\Delta\delta^{13}C$

CMR and SPR shows a different pattern at different soil series and climatic zones. C mineralization per kg of soil (CMR) increased with latitude along the gradient transect, (n=70, R^2=0.38, and p<0.0001) (Fig. 3) showing discreet significant differences among soil series. Los Vilos at 31.9°S in MSA climatic zones exhibit the lowest CMR, increasing slightly southwards to Agua Fresca y Santa Olga soil series at 53.2°S and 53.3°S in a climatic zone SPD. On the other hand, SPR per unit of C exhibit the highest values at the extremes of the latitudinal gradient, Los Vilos (31.9°S) and Agua Fresca (53.2°S) in MSA and SPD climatic zones respectively; and the lowest values in the soil series Bramaderos (35.8°S), Santa Bárbara (36.6°S), Mayamó (42.1°S) and Aituí (43.1°S) from the central section of the latitudinal gradient with TSO and TO climatic zones (n=70, R^2=0.23, and p=0.0018). Displaying a Gaussian distribution (Figure 3 and Table 3). Moreover, CMR and SPR in the soil profile, both decreased as soil depth increases (Table 4). CMR ranged from 0.46 to 15.82 (mg CO_2-C kg $soil^{-1}$ day^{-1}) with an average of 4.88 (±5.25 S.D.) mg CO_2-C kg $soil^{-1}$ day^{-1} in the 0-5 cm depth. In the 40-60 cm depth increment ranged from 0.11 to 0.62 mg CO_2-C kg $soil^{-1}$ day^{-1}, with an average of 0.29 (±0.18 S.D.) mg CO_2-C kg $soil^{-1}$ day^{-1} (Table 3). SPR ranged from 0.01 to 0.22 mg CO_2-C kg $soil^{-1}$ day^{-1}, with an average of 0.06 (±0.06 S.D.) mg CO_2-C kg $soil^{-1}$ day^{-1}in the 0-5 cm depth. In the 40-60 cm depth increment ranged from $2.0E^{-03}$ to 0.05 with an average of 0.02 (±0.02 S.D.) mg CO_2-C kg $soil^{-1}$ day^{-1} (Table 3).

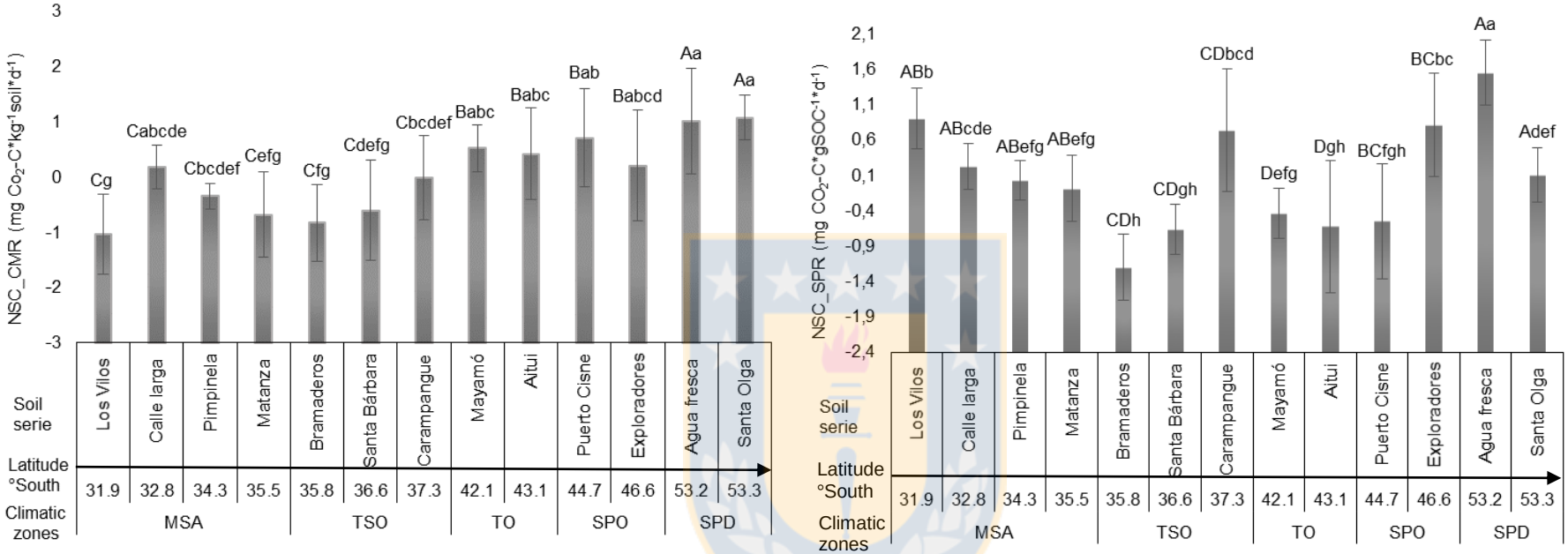

Fig. 3 Latitudinal gradient (degrees S) of C mineralization rate (CMR) (mg CO_2-C kg $soil^{-1}$ d^{-1}) and the Specific potential respiration (SPR) (mg CO_2-C kg $soil^{-1}$ d^{-1}) over all soil samples analysed at different soil depths (from 0 to 60 cm). Significant differences ($p < 0.05$) of Normal Score CMR and SPR transformed data are indicated by Capital letter for mean comparison between climatic zones (CMR n=70, R^2=0.38, p<0.0001; SPR, n=70, R^2=0.23, p=0.0018) and lowercase letter for soil series mean comparison (CMR, n=70, R^2=0.49, p<0.0001; SPR, n=70, R^2=0.66, p<0.0001).

The analysis of the relationship between $\Delta\delta^{13}C$ values and C mineralization rates from 0 to 60 cm depth performed across all sampled revealed a positive regression model (R^2= 0.62 p<0.0001). Similar, a positive relationship between $\Delta\delta^{13}C$ values and SPR is observed (R^2= 0.29 p<0.01) for all soil depths in both cases (Fig. 4 and 5).

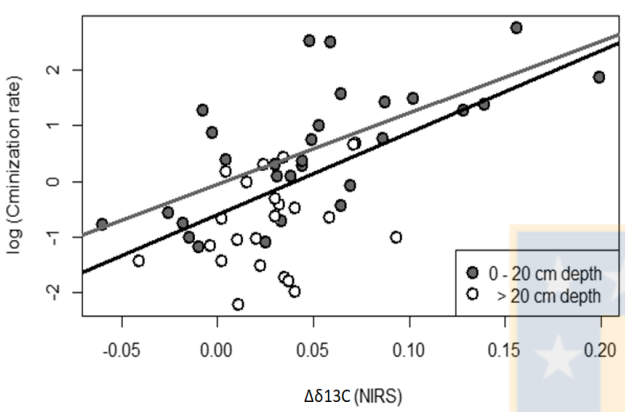

Fig. 4 Relationship between log-transformed C mineralization rate (CMR) and the corresponding $\Delta\delta^{13}C$ values using linear regression for samples <20cm soil depth (black line) (n=30; p-value < 0.0001, R^2= 0.68) and for samples > 20cm depth datapoints (grey line) (n=22, R^2 = 0.62, p-value = 0.0001).

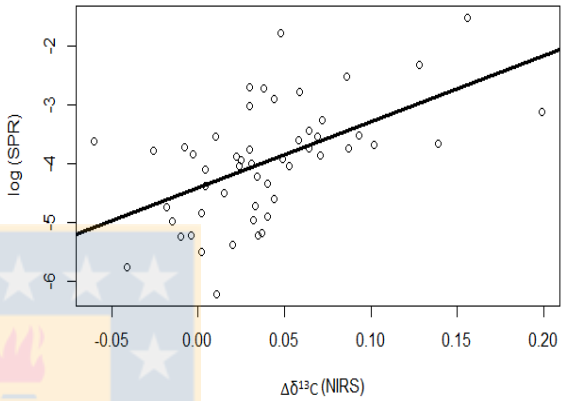

Fig. 5 Relationship between log-transformed Specific potential respiration (SPR) and the corresponding $\Delta\delta^{13}C$ values using linear regression for all datapoints (n= 52, R^2= 0.29, p-value < 0.01).

3.3 Controls on $\Delta\delta^{13}C$ and its relationship to predict CMR and SPR

The result from partial correlation analysis shows significant Pearson correlations for zero order correlations between $\Delta\delta^{13}C$ and CMR when all soil depths (r=0.57) are included (Table 5). This correlation was unaffected by including partial controls related to SOC (r=0.50), MAP (r=0.59) and

physical/chemical variables (SOC, clay content, pH, KCl, Fe and Al content) (r=0.56).

Table 5. Correlation between C mineralization rate (CMR) with $\Delta\delta^{13}C$ as zero order and when controlled by soil %C, MAP as climate variable and physical/chemical (clay, pH, Fe and Al). Significance of the correlations (∗) is evaluated at $p < 0.05$. Depth increments; all (n=26); 0-10 cm (n=10); 10-30 cm (n=10); 30-60 cm (n=6).

	Controlling variables			
Depth increment (cm)	Zero-order	soil C	MAP	phy/chem
all	**0.57***	**0.50***	**0.59***	**0.56***
0 - 10	0.55	0.49	0.57	**0.54***
10 - 30	0.52	0.66	**0.68***	**0.52***
30 - 60	-0.23	0.24	-0.24	-0.25

Table 6. Correlation between Specific potential respiration (SPR) with $\Delta\delta^{13}C$ as zero order and when controlled by soil %C, MAP as climate variable and physical/chemical (clay, pH, Fe and Al). Significance of the correlations (∗) is evaluated at $p < 0.05$. Depth increments; all (n=26); 0-10 cm (n=10); 10-30 cm (n=10); 30-60 cm (n=6).

	Controlling variables			
Depth increment (cm)	Zero-order	soil C	MAP	phy/chem
all	**0.51***	**0.54***	**0.49***	**0.48***
0 - 10	0.43	0.53	0.42	**0.39***
10 - 30	0.62	**0.69***	0.61	**0.60***
30 - 60	0.11	0.00	0.12	0.21

Similar, when analysing separated depth increments only, correlations remain similar with a slight increase in significance when controlling the above-mentioned variables. In the same way, correlations across all soil depths

between $\Delta\delta^{13}C$ and SPR were significant for both zero order (r=0.51) as well as when being controlled for SOC content (r=0.54), MAP (0.49) and physical/chemical variables (r=0.48). When analysing separate depth increments controlling for soil C and physico-chemical variables increased the level of significance but, correlation fit between variables remained similar (Table 6). Note that the above-described trends for separate depth increments were not observed for the deepest depth increment (30-60 cm) for which no significant correlations were found.

4. DISCUSSION

4.1 Evolution of the $\delta^{13}C$ signature at the geo-latitudinal transect, and of SOM, CMR and SPR in the soil profile

We observed a significant difference ($p<0.05$) in the enrichment $\delta^{13}C$ among climatic zones trough the latitudinal gradient. Where, the highest $\delta^{13}C$ was found in the upper north part of the gradient in MSA climatic zone with decreasing $\delta^{13}C$ value toward the template and subpolar climates zones (Fig. 2). This result indicates that climatic conditions in combination with soil mineralogy influence the natural abundance of $\delta^{13}C$ in the soil across larger scales. In the same way, the differences in the results observed for CMR and SPR through the latitudinal gradient (Fig. 3) confirms the effects of climate and soil geochemistry on the C decomposition. As, CMR exhibit a clear significant difference ($p<0.10$) among climatic zones from north to south in the geo latitudinal transect, showing the

effect of climate on CMR. Climate has been reported to indirectly affect soil carbon stock by determining plant productivity and C detritus inputs (Bird et al. 2002; Davidson, 2015), but also affecting rates of enzymatic microbial decomposition (Sinsabaugh, 2010; Wang et al. 2018), mineral weathering and modifying geochemical properties (Doetterl et al. 2018; Hunter et al. 1998; Singh et al. 2017) which are linked to mineral related stabilization processes (Davidson, 2015). Doetterl et al. (2015) demonstrated that the interactions of climatic and geochemical factors control soil organic carbon storage and turnover in grasslands. However; soil organic C density (SOCD or C stock) and its driving factors are also depending of the ecosystems and soil depth examined (Wang et al. 2013; Guan et al. 2019). Wang et al. (2013) concluded that SOCD is a key contributor to the variation of soil $\delta^{13}C$; their results showed that soil organic carbon and $\delta^{13}C$ were correlated with soil characteristics across different ecosystems (e.g. forest; meadow; steppe; croplands). In a different way, the result for SPR through the latitudinal gradient (Fig. 3) present a Gaussian distribution with higher values of SPR in the extremes of the transect and lower ones in the centre of the transect. The extremes areas of the transect correspond to those with lower MAP, lower C content and sandy loam soil types (Table 1 and 2). Unlike the central part of the transect that exhibit the higher MAP, soil C content and more enriched in aluminosilicate secondary mineral soil types (Table 1 and 2). Characteristics that indicate a higher dependence of soil mineralogy and C stabilization factors influencing on SPR. As reported by Doetterl et al. (2015) in the same geolatitudinal transect, the MSA and SPD part of the gradient segment are the zones described with harsh conditions with

dominant mechanical weathering, increasing specific C respiration and decreasing SOC stock. In these conditions a further ^{13}C enrichment trough isotopic fractionation can be expected (Feng, 2002; Poage & Feng, 2004; Tcherkez et al. 2011; Wang et al. 2018; Wynn et al. 2005). At the same time differences in $\delta^{13}C$ with depth are less under those climatic conditions (Fig. 3) as soils have a generally lower capacity of mineral C stabilization (Dotterl et al. 2015). Similar, Poage & Feng (2004) describe mean annual temperature, soil moisture and soil chemistry as environmental factors influencing the C microbial discrimination.

Our results on the evolution of the $\delta^{13}C$ signature of SOM, indicating a progressive enrichment of ^{13}C in SOM with soil depth in parallel to decreasing C content with depth are shown in Fig. 2. In agreement with previous studies (Accoe et al. 2003; Acton et al. 2013; Feng, 2002; Poage and Feng, 2004). The enrichment of ^{13}C with depth is likely to be explained with kinetic isotopic fractionation (e.g., Accoe et al. 2003), intrinsic to microbial processes during C decomposition. Kinetic isotope fractionation is further related to a substitution of a heavier isotope for a lighter one that causes a change in the equilibrium constant of a reaction (Rishavy and Cleland, 1998). The microbial discrimination against one isotope by enzymatic catalysis are due to slight differences in bond energy between ^{12}C and ^{13}C isotopologues of substrates and transition states. Then, the preferential use of ^{12}C should lead to a ^{13}C enrichment of OC (Tcherkez et al. 2011). Furthermore, beside the described Suess Effect and paleoclimatic events with possible vegetation changes (Krull et al. 2006). Bird et

al. (2002) and Wynn et al. (2005) have reported an association between 13C enrichment OC with fine mineral particles in fine-textured soils. Where the enriched $\delta^{13}C$ SOM from the microbial fractionation is subjected to stabilization processes by adsorption onto soil mineral phase (aluminosilicate secondary minerals, Al and Fe oxide content) and illuviation processes (Krull et al. 2006), as well as, protected by occlusion in soil aggregates (Di and Huang, 2021; Krull et al. 2006) contributing to the enrichment of $\delta^{13}C$ in the soil profile as soil depth increases. As described earlier, the residual increase in $\delta^{13}C$ of the organic matter below a soil depth of 20 cm can result from the increased contribution of ^{13}C-enriched microbially derived C with depth (Boström et al. 2007).

4.2 Potential C dynamics based on the ^{13}C enrichment in the soil profile

Total soil C content, CMR and SPR, as well as the change of NIRS predicted $\delta^{13}C$ value per depth increment ($\Delta\delta^{13}C$ values) all decreased with soil depth (Table 4) across soils of the entire latitudinal transect. This result confirms many earlier studies which describe that higher SOC decomposition rates occur in topsoil than in subsoil (Accoe et al. 2003; Bailey et al. 2019; Davidson, 2015; Rey et al. 2008). These patterns are often driven by the availability of C to microbial decomposers. In subsoil, the fraction of mineral protected C is usually much higher than in comparable topsoil (Rey et al. 2008), leading to lower CMR, higher C stability and a greater $\Delta\delta^{13}C$ values with depth (Accoe et al. 2003).

Linear regression across all data points, as well as for isolated topsoil and for shallow subsoil samples show that $\Delta\delta^{13}C$ values are significantly correlated to CMR and SPR indicating that $\Delta\delta^{13}C$ can be used to indicate C degradability

(Fig. 4 and 5, Table 5 and 6). However, when analysing correlation between the above-mentioned parameters for deeper subsoil (30-60cm) alone no significant correlations were found (Table 5 and 6). Similar, results from the partial correlation analysis confirm that controlling for the variation in major soil or climatic variables does not significantly improve correlations between $\Delta\delta^{13}C$, respiration or mineralization (Table 5 and 6). Thus, while depth trends of C turnover can be explained using $\Delta\delta^{13}C$, variation between sites in deeper subsoil are controlled by variation in site parameters that are not covered by our analyses or beyond the precision of our NIRS based assessment method. Nevertheless, uncertainty and variability in the prediction power of our model reveals the importance of considering the latitudinal changeability in soil types as a control on properties controlling $\Delta\delta^{13}C$.

5. CONCLUSIONS

In summary, $\delta^{13}C$ enrichment along the transect was observed for dry climate zones and with soil depth. Our analysis shows that $\Delta\delta^{13}C$ values can serve as an indicator of the potential degradability of SOM under permanent temperate grassland and may be used as a predictor in the relationship between CMR and SPR with the soil C isotope. Thus, estimates of NIRS derived soil $\Delta\delta^{13}C$ values have the potential to become an easily applicable and cost-effective technique to estimate soil C degradability under different geo-climatic conditions. These results indicate the importance of local calibration with precise soil data on

confounding controlling variables and the importance of understanding potential controls on local scale SOC dynamics, and decomposition processes. Overall, our results show both the relevance of identifying critical zones to understand C dynamics in a variable environmental condition and the need for prediction of CMR and SPR, in order to understand the impact of climate change effects. Furthermore, the use of a reliable and low-cost methodology to estimate C decomposition, avoiding the time consuming and sample disturbing when using soil incubation techniques become clear.

Acknowledgements We acknowledge the kind help of Katherine Rebolledo for laboratory work support, Juan Fuentes and Professor's Manuel Casanova's team for field work support during the soil sampling campaign,

Author Contributions: Conceptualization: M.H., C.M., M.C., S.D., P.B., and E.Z; methodology: MH., M. de los Á.S., M.C., S.B., P.B., and E.Z.; formal analysis and investigation: M.H., DW., S D, and E.Z.; writing—original draft: M.H.; writing—review and editing S.D., D.W., C M., M.C., S.B., and E.Z.; supervision: E. Z., S.D. All the authors have read the manuscript and agreed to submit it in its current form for publication in the Journal

Funding: This work was supported by Conicyt/Fondecyt Regular Project N°1161492, and the Agronomy Sciences Doctoral Program of the Faculty of Agronomy, Universidad de Concepción.

Declarations

Conflict of interest

The authors declare that they have no conflict of interest.

6 REFERENCES

Accoe F, Boeckx P, Cleemput O. V, Hofman G, Zhang Y, Li R. H, & Guanxiong C (2002) Evolution of the $\delta^{13}C$ signature related to total carbon contents and carbon decomposition rate constants in a soil profile under grassland. Rapid Communications in Mass Spectrometry 16(23), 2184-2189. https://doi.org/10.1002/rcm.767

Accoe F, Boeckx P, Cleemput O. V, & Hofman G. (2003) Relationship between soil organic C degradability and the evolution of the $\delta^{13}C$ signature in profiles under permanent grassland. Rapid Communications in Mass Spectrometry 17(23), 2591-2596. DOI:10.1002/rcm.1202

Acton P, Fox, J, Campbell E, Rowe H, & Wilkinson M. (2013) Carbon isotopes for estimating soil decomposition and physical mixing in well-drained forest soils. Journal of Geophysical Research: Biogeosciences 118(4), 1532-1545.

Ågren G. I, E. Bosatta and J. Balesdent (1996) Isotope discrimination during decomposition of organic matter: A theoretical analysis. Soil Sci. Soc. Am. J., 60, 1121– 1126. DOI:10.1002/2013JG002400

Arora V. K, Boer G. J, Friedlingstein P, Eby M, Jones C. D, Christian J. R, ... & Wu T. (2013) Carbon–concentration and carbon-climate feedbacks in CMIP5 Earth system models. Journal of Climate 26(15), 5289-5314. DOI: 10.1175/JCLI-D-12-00494.1

Balesdent J, & Mariotti A. (1996) Measurement of soil organic matter turnover using ^{13}C natural abundance. Mass spectrometry of soils 41(3), 83-111.

Balesdent J, Basile-Doelsch I, Chadoeuf J. et al. (2018) Atmosphere–soil carbon transfer as a function of soil depth. Nature 559, 599–602. https://doi.org/10.1038/s41586-018-0328-3

Bailey V. L, Pries C. H, & Lajtha K. (2019) What do we know about soil carbon destabilization? Environmental Research Letters 14(8), 083004. https://doi.org/10.1088/1748-9326/ab2c11

Bird M. I, & Pousai P. (1997) Variations of $\delta^{13}C$ in the surface soil organic carbon pool. Global Biogeochemical Cycles 11(3), 313-322.

Bird M. I, Santruckova H., Arneth A., Grigoriev S, Gleixner G, Kalaschnikov Y. N, ... & Schulze E. D. (2002) Soil carbon inventories and carbon-13 on a latitude transect in Siberia. Tellus B: Chemical and Physical Meteorology 54(5), 631-641. https://doi.org/10.3402/tellusb.v54i5.16699

Bird M, Kracht O., Derrien D, & Zhou Y. (2003) The effect of soil texture and roots on the stable carbon isotope composition of soil organic carbon. Soil Research 41(1), 77-94. DOI: 10.1071/SR02044

Blake G. R, & Hartge K. H. (1986) Particle density. Methods of soil analysis: Part 1 physical and mineralogical methods 5, 377-382. https://doi.org/10.1002/gea.3340050110https://doi.org/10.1002/gea.3340050110

Boström B, Comstedt D, & Ekblad A. (2007) Isotope fractionation and ^{13}C enrichment in soil profiles during the decomposition of soil organic matter. Oecologia 153(1), 89-98. DOI 10.1007/s00442-007-0700-8

Bouyoucos G. J. (1962) Hydrometer method improved for making particle size analysis of soils. Agron. J. 54, 464–465. https://doi.org/10.2134/agronj1962.00021962005400050028x

Boutton T. W. (1991) Stable carbon isotope ratios of natural materials: I. Sample preparation and mass spectrometric analysis. in Carbon isotope techniques 1, 155. DOI: 10.1016/B978-0-12-179730-0.50021-7

Boutton T. W. (1996) Stable carbon isotope ratios of soil organic matter and their use as indicators of vegetation and climate change, T W Boutton S I Yamasaki (Eds). In: Mass Spectrometry of Soils, Marcel Dekker, New York, pp 47–82.

Brugnoli E, & Farquhar G. D. (2000) Photosynthetic fractionation of carbon isotopes. In Photosynthesis (pp. 399-434). Springer, Dordrecht. https://doi.org/10.1007/0-306-48137-5_17

Brunn M, Spielvogel S, Sauer, T, & Oelmann Y. (2014) Temperature and precipitation effects on $\delta^{13}C$ depth profiles in SOM under temperate beech forests. Geoderma, 235, 146-153. DOI:10.1016/J.GEODERMA.2014.07.007

Cutler, A., Cutler, D.R. and Stevens, J.R. (2012) Random forests. In: Zhang, C. and Ma, Y.Q., Eds., Ensemble Machine Learning, Springer, Boston, MA. http://dx.doi.org/10.1007/978-1-4419-9326-7_5

Dahlgren, R. A, Saigusa, M, & Ugolini F. C. (2004). Nature, properties and management of volcanic soils. Advances in agronomy 82(03), 113-182. DOI:10.1016/S0065-2113(03)82003-5

Davidson E. A. (2015) Biogeochemistry: Soil carbon in a beer can. Nature Geoscience 8(10), 748-749. https://doi.org/10.1038/ngeo2522

Di D. R, & Huang G. W. (2021) Isotope analysis reveals differential impacts of artificial and natural afforestation on soil organic carbon dynamics in

abandoned farmland. Plant and Soil 1-14. https://doi.org/10.1007/s11104-021-05243-x

Dwivedi D., Riley W. J, Torn M. S, Spycher N, Maggi F, & Tang J. Y. (2017) Mineral properties, microbes, transport, and plant-input profiles control vertical distribution and age of soil carbon stocks. Soil Biology and Biochemistry 107, 244-259. https://doi.org/10.1016/j.soilbio.2016.12.019

Doetterl S, Stevens A, Six J, Merckx R, Van Oost K, Pinto M. C, ... & Boeckx P. (2015) Soil carbon storage controlled by interactions between geochemistry and climate. Nature Geoscience 8(10), 780-783. https://doi.org/10.1038/ngeo2516

Doetterl S, Berhe A. A, Arnold C, Bodé S, Fiener P, Finke P, et al. (2018) Links among warming, carbon and microbial dynamics mediated by soil mineral weathering. Nature Geoscience 11(8), 589. https://doi.org/10.1038/s41561-018-0168-7

Fuentes M, Hidalgo C, González-Martín I, Hernández-Hierro J. M, Govaerts B, Sayre K. D, & Etchevers J. (2012) NIR spectroscopy: an alternative for soil analysis. Communications in Soil Science and Plant Analysis 43(1-2), 346-356. https://doi.org/10.1080/00103624.2012.641471

Feng X. (2002) A theoretical analysis of carbon isotope evolution of decomposing plant litters and soil organic matter. Global Biogeochemical Cycles16(4),66-1. https://doi.org/10.1029/2002GB001867https://doi.org/10.1029/2002GB001867

Gleixner G, Poirier N, Bol R, & Balesdent J. (2002) Molecular dynamics of organic matter in a cultivated soil. Organic geochemistry 33(3), 357-366. https://doi.org/10.1016/S0146-6380(01)00166-8

Goovaerts P. (2001) Geostatistical modelling of uncertainty in soil science. Geoderma 103(1-2), 3-26. https://doi.org/10.1016/S0016-7061(01)00067-2

Guan J. H, Deng L, Zhang J. G, He Q. Y, Shi W. Y, Li G, & Du S. (2019). Soil organic carbon density and its driving factors in forest ecosystems across a northwestern province in China. Geoderma, 352, 1-12. https://doi.org/10.1016/j.geoderma.2019.05.035

Högberg P, Ekblad A, Nordgren A, Plamboeck A. H, Ohlsson A, Bhupinderpal-Singh S, & Högberg M. (2005) Factors determining the ^{13}C abundance of soil-respired CO2 in boreal forests. Elsiever p. 47 – 68. DOI: 10.1016/B978-012088447-6/50004-0

Hunter K. S, Wang, Y, & Van Cappellen P. (1998) Kinetic modeling of microbially-driven redox chemistry of subsurface environments: coupling transport, microbial metabolism and geochemistry. Journal of hydrology209(1-4), 53-80. https://doi.org/10.1016/S0022-1694(98)00157-7https://doi.org/10.1016/S0022-1694(98)00157-7

Hunter K. S, Wang Y, & Van Cappellen, P. (1998) Kinetic modeling of microbially-driven redox chemistry of subsurface environments: coupling transport, microbial metabolism and geochemistry. Journal of hydrology 209(1-4), 53-80. https://doi.org/10.1016/S0022-1694(98)00157-7

Jackson R. B, Le Quéré C, Andrew R. M, Canadell, J. G, Peters G. P, Roy J, & Wu L. (2017) Warning signs for stabilizing global CO2 emissions. Environmental Research Letters 12(11), 110 202. https://doi.org/10.1088/1748-9326/aa9662

Jones C, McConnell C, Coleman K, Cox P, Falloon P, Jenkinson D, & Powlson D. (2005) Global climate change and soil carbon stocks; predictions from two contrasting models for the turnover of organic carbon in soil. Global Change Biology, 11(1), 154-166. https://doi.org/10.1111/j.1365-2486.2004.00885.x

Jones D. L, Kielland K, Sinclair F. L, Dahlgren R. A, Newsham K. K, Farrar J. F, & Murphy D. V. (2009) Soil organic nitrogen mineralization across a global latitudinal gradient. Global Biogeochemical Cycles 23(1). https://doi.org/10.1029/2008GB003250

Krull E. S, Bestland E. A, Skjemstad J. O, & Parr J. F. (2006) Geochemistry ($\delta^{13}C$, $\delta^{15}N$, ^{13}C NMR) and residence times (14C and OSL) of soil organic matter from red-brown earths of South Australia: Implications for soil genesis. Geoderma 132(3-4), 344-360. https://doi.org/10.1016/j.geoderma.2005.06.001

Kuzyakov Y, Biriukova O, Turyabahika F, & Stahr K. (2001) Electrostatic method to separate roots from the soil. Journal of Plant Nutrition and Soil Science 164(5),541-545. https://doi.org/10.1002/1522-2624(200110)164:5<541::AID-JPLN541>3.0.CO;2-H

Lefèvre C, Rekik F, Alcantara V, & Wiese L. (2017) Carbono Orgánico del Suelo: el potencial oculto. Available via DIALOG. http://www.fao.org/3/b-i6937s.pdf

Lichtfouse E, Lichtfouse M, & Jaffrézic A. (2003) $\delta^{13}C$ values of grasses as a novel indicator of pollution by fossil-fuel-derived greenhouse gas CO2 in urban areas. Environmental science & technology 37(1), 87-89. https://doi.org/10.1021/es025979yhttps://doi.org/10.1021/es025979y

Liu S, Li Y, Wu J, Huang D, Su Y, & Wei W. (2010) Spatial variability of soil microbial biomass carbon, nitrogen and phosphorus in a hilly red soil landscape in subtropical China. Soil science and plant nutrition 56(5), 693-704. https://doi.org/10.1111/j.1747-0765.2010.00510.x

Luo Y, Ahlström A, Allison S. D, Batjes N. H, Brovkin V, Carvalhais N, et al. (2016) Toward more realistic projections of soil carbon dynamics by Earth system models. Global Biogeochemical Cycles 30(1), 40-56. https://doi.org/10.1002/2015GB005239

Luo Z, Feng W, Luo Y, Baldock J, & Wang E. (2017) Soil organic carbon dynamics jointly controlled by climate, carbon inputs, soil properties and soil carbon fractions. Global Change Biology 23(10), 4430-4439. https://doi.org/10.1111/gcb.13767

Martens, H. and Naes, T. 1989. Multivariate calibration Johnson Wiley & Sons, Chichester.

Piotrowska N, Pazdur A, Pawełczyk S, Rakowski A. Z, Sensuła B, & Tudyka K. (2020) Human Activity Recorded in Carbon Isotopic Composition of Atmospheric CO 2 in Gliwice Urban Area and Surroundings (Southern Poland) in the Years 2011–2013. Radiocarbon 62(1), 141-156. https://doi.org/10.1017/RDC.2019.92

Poage M. A, & Feng X. (2004) A theoretical analysis of steady-state $\delta^{13}C$ profiles of soil organic matter. Global biogeochemical cycles 18(2). https://doi.org/10.1029/2003GB002195

Powers J. S, & Schlesinger W. H. (2002) Geographic and vertical patterns of stable carbon isotopes in tropical rain forest soils of Costa Rica. Geoderma 109(1-2), 141-160. https://doi.org/10.1016/S0016-7061(02)00148-9

Ramírez P. B, Calderón F. J, Fonte S. J, Santibáñez F, & Bonilla C. A. (2020) Spectral responses to labile organic carbon fractions as useful soil quality indicators across a climatic gradient. Ecological Indicators 111, 106042. https://doi.org/10.1016/j.ecolind.2019.106042

Rey A, Pegoraro E, & Jarvis P. G. (2008) Carbon mineralization rates at different soil depths across a network of European forest sites (FORCAST). European Journal of Soil Science 59(6), 1049-1062. https://doi.org/10.1111/j.1365-2389.2008.01065.x

Rinnan, A., Van den Berg, F., Engelsen, B. 2009. Review of the most common pre-processing techniques for near-infrared spectra. Trends in Analytical Chemestry 28 (10): 1201–1222. https://doi.org/10.1016/j.trac.2009.07.007

Rishavy M. A, & Cleland W. W. (1999) ^{13}C, ^{15}N, and ^{18}O equilibrium isotope effects and fractionation factors. Canadian Journal of Chemistry 77(5/6), 967.

Robertson A. D, Paustian K, Ogle S, Wallenstein M. D, Lugato E, & Cotrufo M. F. (2019) Unifying soil organic matter formation and persistence frameworks: the MEMS model. Biogeosciences 16(6), 1225-1248. https://doi.org/10.5194/bg-16-1225-2019

Rumpel C, & Kögel-Knabner I. (2011) Deep soil organic matter—a key but poorly understood component of terrestrial C cycle. Plant and soil 338(1), 143-158. https://doi.org/10.1007/s11104-010-0391-5

Sheikh M. A, Kumar M, Todaria N. P, & Pandey R. (2020) Biomass and soil carbon along altitudinal gradients in temperate Cedrus deodara forests in Central Himalaya, India: Implications for climate change mitigation. Ecological Indicators 111, 106025. https://doi.org/10.1016/j.ecolind.2019.106025

Schimel D. S, Braswell B. H, Holland E. A, McKeown R, Ojima D. S, Painter T. H, et al. (1994) Climatic, edaphic, and biotic controls over storage and turnover of carbon in soils. Global biogeochemical cycles 8(3), 279-293. https://doi.org/10.1029/94GB00993

de los Ángeles Sepúlveda M, Hidalgo M, Araya J, Casanova M, Muñoz C, Doetterl S, et al. (2021) Near-infrared spectroscopy: Alternative method for assessment of stable carbon isotopes in various soil profiles in Chile. Geoderma Regional 25, e00397. https://doi.org/10.1016/j.geodrs.2021.e00397

Singh M, Sarkar B, Sarkar S, Churchman J, Bolan N, Mandal S, et al. (2018) Stabilization of soil organic carbon as influenced by clay mineralogy. In Advances in agronomy. Academic Press Vol. 148, pp. 33-84.. https://doi.org/10.1016/bs.agron.2017.11.001

Sinsabaugh R. L. (2010) Phenol oxidase, peroxidase and organic matter dynamics of soil. Soil Biology and Biochemistry 42(3), 391-404. https://doi.org/10.1016/j.soilbio.2009.10.014

Tcherkez G, Mahé A, & Hodges M. (2011) $^{12}C/^{13}C$ fractionations in plant primary metabolism. Trends in plant science 16(9), 499-506. https://doi.org/10.1016/j.tplants.2011.05.010https://doi.org/10.1016/j.tplants.2011.05.010

Van der Watt H. V. H, & Van Rooyen T. H. (1990) A glossary of soil science. Soil Science Society of South Africa.

Wallander H, Göransson H, & Rosengren U. (2004) Production, standing biomass and natural abundance of ^{15}N and ^{13}C in ectomycorrhizal mycelia collected at different soil depths in two forest types. Oecologia 139(1), 89-97. DOI 10.1007/s00442-003-1477-z

Wang S, Fan J, Song M, Yu G, Zhou L, Liu J, ... & Song T. (2013) Patterns of SOC and soil ^{13}C and their relations to climatic factors and soil characteristics on the Qinghai–Tibetan Plateau. Plant and Soil 363(1), 243-255. DOI 10.1007/s11104-012-1304-6

Wang C, Wei H, Liu D, Luo W, Hou J, Cheng, et al. (2017) Depth profiles of soil carbon isotopes along a semi-arid grassland transect in northern China. Plant and Soil 417(1), 43-52. https://doi.org/10.1007/s11104-017-3233-x

Wang C, Houlton B. Z, Liu D, Hou J, Cheng W, & Bai E. (2018) Stable isotopic constraints on global soil organic carbon turnover. Biogeosciences 15(4), 987-995. https://doi.org/10.5194/bg-15-987-2018

Winowiecki L. A, Vågen T. G, Boeckx P, & Dungait J. A. (2017) Landscape-scale assessments of stable carbon isotopes in soil under diverse vegetation classes in East Africa: application of near-infrared spectroscopy. Plant and Soil 421(1-2), 259-272. https://doi.org/10.1007/s11104-017-3418-3

Wynn J. G, Bird M. I, & Wong V. N. (2005) Rayleigh distillation and the depth profile of $^{13}C/^{12}C$ ratios of soil organic carbon from soils of disparate texture in Iron Range National Park, Far North Queensland, Australia. Geochimica et cosmochimica acta 69(8), 1961-1973. https://doi.org/10.1016/j.gca.2004.09.003

Zagal E, Muñoz C, Espinoza S, & Campos J. (2012) Soil profile distribution of total C content and natural abundance of ^{13}C in two volcanic soils subjected to crop residue burning versus crop residue retention. Acta Agriculturae Scandinavica, Section B-Soil & Plant Science 62(3), 263-272. https://doi.org/10.1080/09064710.2011.608707

IV. CAPITULO 4. CONCLUSIONES GENERALES Y PROYECCIONES

La metodología NIRS es una técnica no destructiva y de menor costo que puede ser utilizada para el estudio del C suelo y sus isótopos estables. La calibración y validación de un modelo de predicción de $\delta^{13}C$ basado en datos NIRS utilizando los enfoques de regresión PLS y RF, así lo demuestran. Los parámetros RMSEP de ambos modelos indicaron que la NIRS puede utilizarse para predecir el $\delta^{13}C$ para varios perfiles de suelo. Los rendimientos del modelo fueron elevados para la predicción de muestras mediante NIRS cuando las muestras procedían del mismo conjunto de muestras usados para su construcción y desarrollo. Los resultados de $\delta^{13}C$ del COS obtenidas en este estudio apoyan el uso de la NIRS como método de predicción en el análisis de suelos y como método no destructivo sin residuos para los estudios sobre la dinámica del C en el suelo.

En cuanto a la predictibilidad de $\delta^{13}C$ en los suelos puede estar ligada a su correlación con las propiedades mineralógicas del suelo, tales como el contenido de arcilla y la suma de bases.

Por tanto, los datos de $\delta^{13}C$ derivados de NIRS de los trece sitios de estudio nos permitieron evaluar el uso de los valores de $\Delta\delta^{13}C$ de los perfiles del suelo a lo largo de un transecto latitudinal para evaluar su capacidad de predecir la CMR y la SPR del suelo y, a su vez, la tasa de degradabilidad del C, que según Accoe et al. (2012) indirectamente es una evaluación de su estabilidad.

Se observó un enriquecimiento de $\delta^{13}C$ con el aumento de profundidad en el perfil de suelo. Así como también, a lo largo del transecto, especialmente para

zonas de clima seco. Se encontró una correlación positiva y significativa entre las variables CMR y SPR con $\Delta\delta^{13}C$ para los primeros 20 cm de suelo y los subsuelos poco profundos. En los subsuelos más profundos, no se pudieron encontrar correlaciones significativas entre estas últimas variables.

Nuestro análisis muestra que los valores de $\Delta\delta^{13}C$ pueden servir como un indicador de la degradabilidad (o 'estabilidad potencial') de la MOS bajo praderas naturales permanentes y ser utilizados como un índice en la relación entre CMR y SPR con el isótopo estable del C del suelo. Así, las estimaciones de los valores de $\Delta\delta^{13}C$ del suelo derivadas de NIRS tienen el potencial de convertirse en una técnica fácilmente aplicable y costo efectiva para estimar la degradabilidad del C del suelo bajo diferentes condiciones geoclimáticas. Sin embargo, el modelo de predicción muestra una alta variabilidad en las predicciones de $\Delta\delta^{13}C$ derivadas de NIRS a través de los tipos de suelo a lo largo del transecto latitudinal. Estos resultados indican la importancia de entender los potenciales controles sobre la dinámica del COS en los distintos escenarios medioambientales, y su interacción con la estabilización de C y los procesos de descomposición. Por otro lado, el desarrollo y validación de un modelo usando valores NIR directamente con valores $\delta^{13}C$ en el perfil del suelo, constituiría una evaluación más directa de la estabilidad del C del suelo (k, 'turnover rate'), complementando los resultados de este estudio y para una mejor comprensión de la dinámica del C del suelo y de sus interacciones clima y geología. Además, la generación de modelos separados por 'clase' de sitio podría en gran medida mejorar el comportamiento predictivo del modelo dentro de esa clase.